Microscopy with Slow Electrons

E. Bauer
Department of Physics and Astronomy
Arizona State University

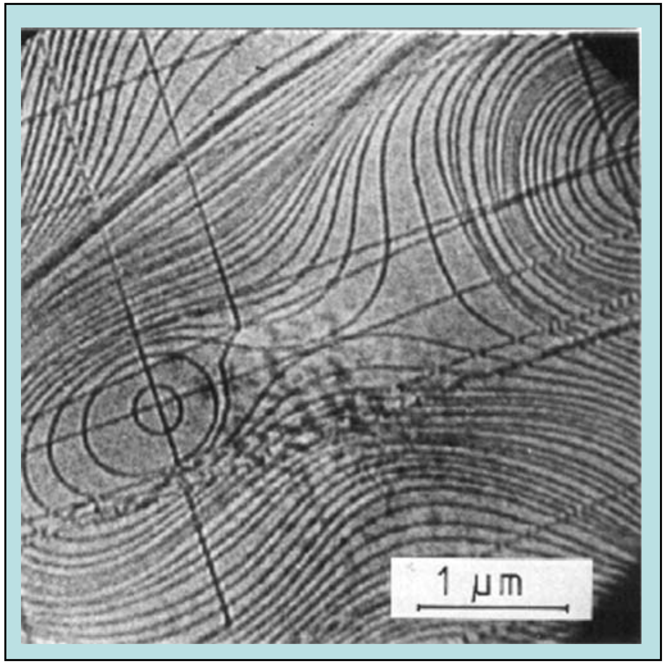

LEEM 1984

XPEEM 2004

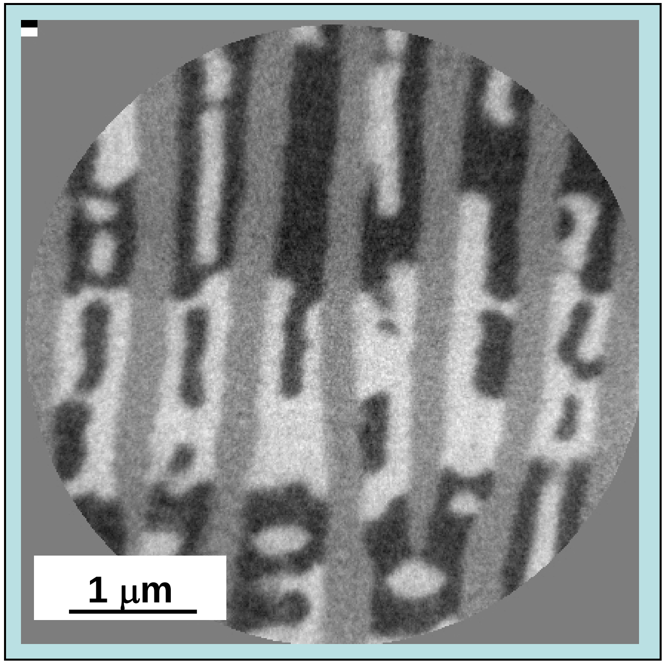

Argonne 09/08/04

Outline

Brief history

Fundamentals of low energy electron optics
- cathode lenses, resolution, transmission, aberration correction

Instruments
- PEEM, LEEM, SPELEEM, SMART

Operation modes
- Imaging, spectroscopy, diffraction

Some applications
- surfactants, magnetic bits, MnAs films

Brief History

<u>Bauer group</u>	Key person
1962 EMSA Philadelphia: LEEM concept (glass system)	
1964-1968 Metal system	George Turner
1978 Leopoldina Symposium: Synchrotron radiation photo emission electron microscopy vs. Auger electron microscopy	
1984 First good LEEM images	Wolfgang Telieps
1988-1992 Spectroscopic PEEM/LEEM (SPELEEM)	Lee Veneklasen
1990 Spin-polarized LEEM (SPLEEM)	Thomas Duden
1996 XPEEM with photo electrons (SPELEEM at ELETTRA)	Thomas Schmidt

<u>Tonner group</u>

1988 XPEEM with secondary electrons (XANES-PEEM)

<u>Stoehr group</u>

1993 XMCDPEEM with secondary electrons

<u>German multi-university group</u>

1994-2004 SMART (aberration-corrected LEEM-PEEM)	Harald Rose

Photo Emission Electron Microscopy (PEEM)

2 types

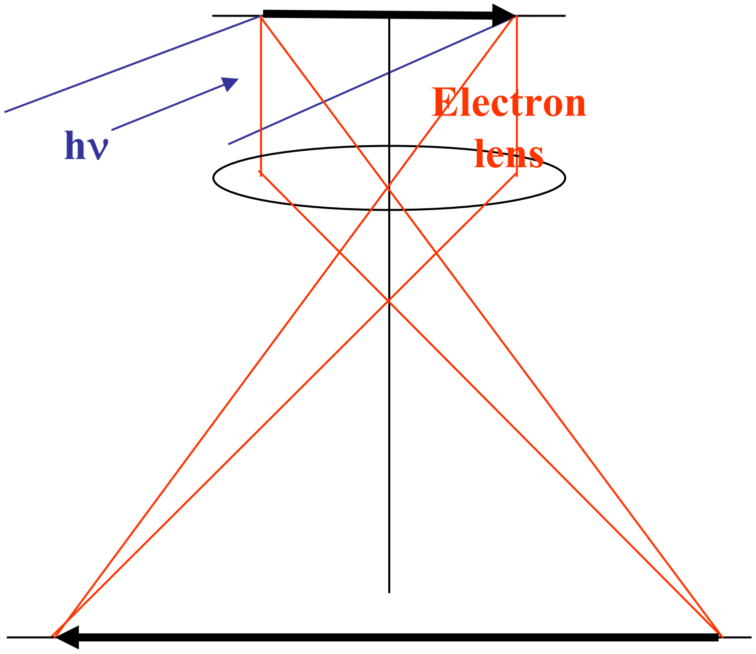

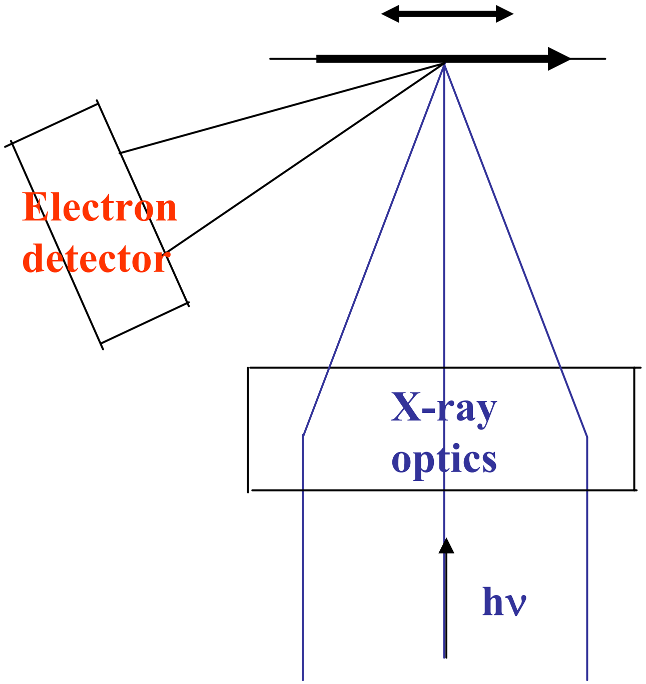

broad illumination

Full field

sample fixed

PEEM

focused illumination

Scanning

sample scanned

The cathode lens

In emission microscopy α is large
Electron lenses can accept only small α because of large chromatic and spherical aberrations
Solution of problem: accelerate electrons to high energy before lens →

Immersion objective lens = cathode lens

$$n \sin\alpha = \text{const}$$
$$n \sim v \sim \sqrt{E}$$
$$\sin\alpha / \sin\alpha_0 = \sqrt{E_0/E}$$

Example for $E = 20000$ eV:

E_0	2 eV	200 eV
$\alpha_0 = 45^o$	$\alpha = 0.4^o$ 7×10^{-3} rad	$\alpha = 4.5^o$ 8×10^{-2} rad

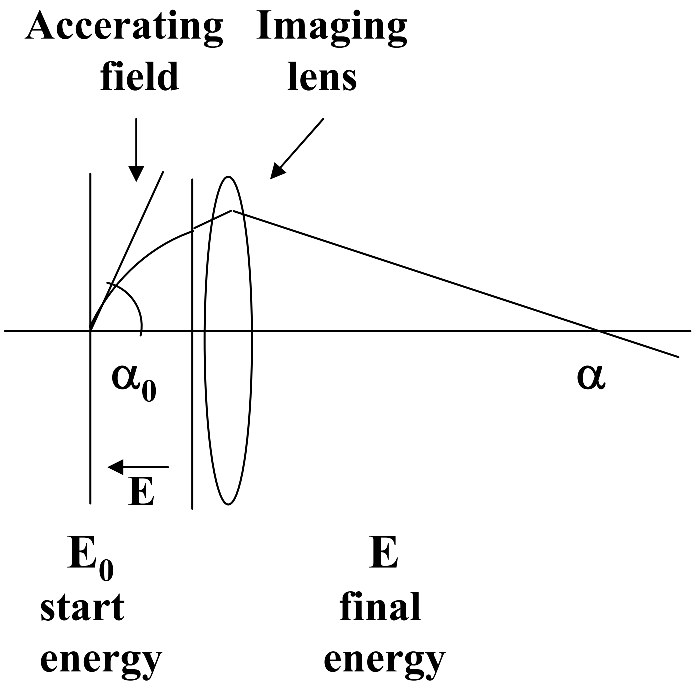

Cathode lens types

Electrostatic tetrode

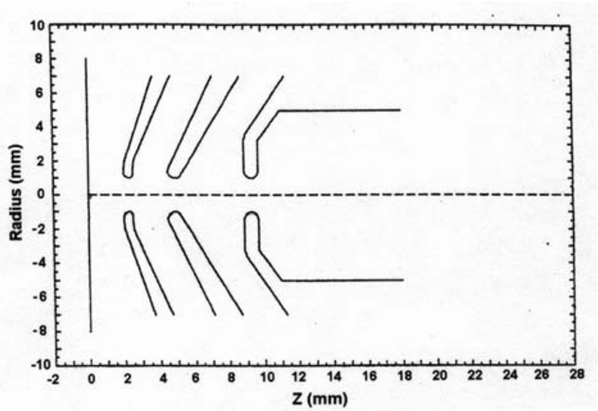

Lens comparison

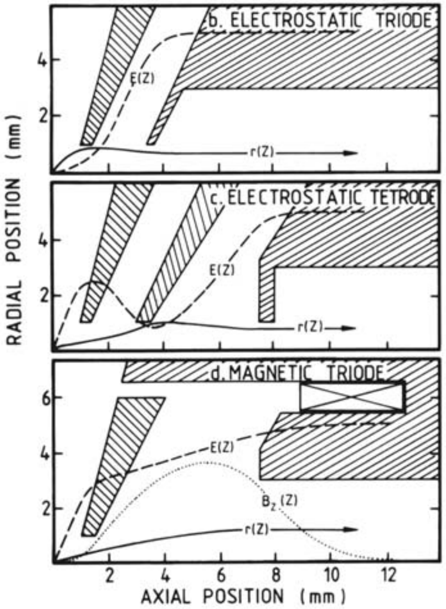

Estimation of aberrations:

Separate lens into acceleration and imaging regions

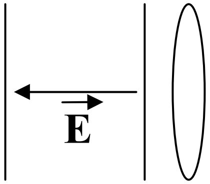

At low energies aberrations of accelerating region dominate

Aberrations of homogeneous acceleration field

$\rho_0 = E_0/E \qquad \varepsilon = \Delta E_0/E \qquad \rho = \rho_0 + \varepsilon$

Spherical aberration $D_{ö}$

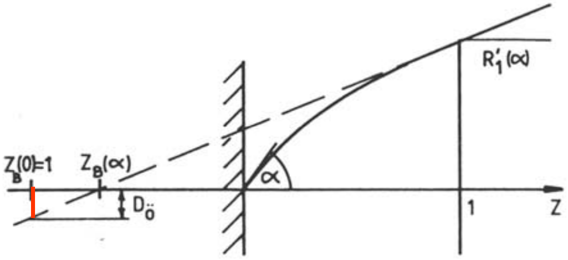

Chromatic aberration D_F

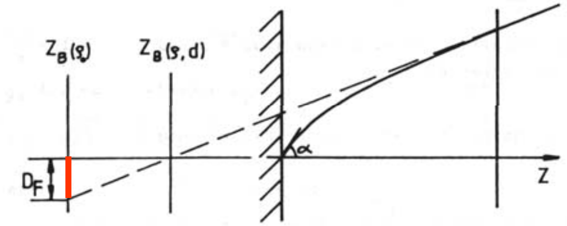

Approximation: ρ_0 and $\varepsilon << 1/\cos \alpha^2 > 1$
Example: $E_0 = 100$ eV, $\Delta E_0 = 1$ eV, $E = 20000$ eV
$\varepsilon = \rho_0 /100, \; \rho_0 = 1/200$

$$D_{ö} \approx 2 \rho \sin \alpha \, (1 - \cos \alpha)$$

$$\approx 2 \rho \quad (\alpha - 1/6\alpha^3)(1/2\alpha^2 - 1/24\, \alpha^4)$$

45^o 10.7%
60^o 17.0%

$\approx \underline{\rho\, \alpha^3}$ **for small α**

overestimation

45^o 20.5%
60^o 36.2%

$$D_F \approx 2 \rho \sin \alpha \, (\sqrt{\rho_0 / \rho} - 1)$$

$\approx \varepsilon \sin \alpha$ **for $\varepsilon << \rho_0$**

$\approx \varepsilon\, (\alpha - 1/6\, \alpha^3)$

Error
45^o 0.3%
60^o 1.2%

$\approx \underline{\varepsilon\, \alpha}$ **for small α**

overestimation

45^o 11.1%
60^o 17.3%

α-dependent aberrations require α-limitation by angle-limiting aperture (“contrast aperture”) with radius r_A

Diffraction by aperture: diffraction disc of confusion $d_B = 0.6\, \lambda / r_A$

Approximate resolution $d = \sqrt{d_{\ddot{o}}^2 + d_F^2 + d_B^2}$

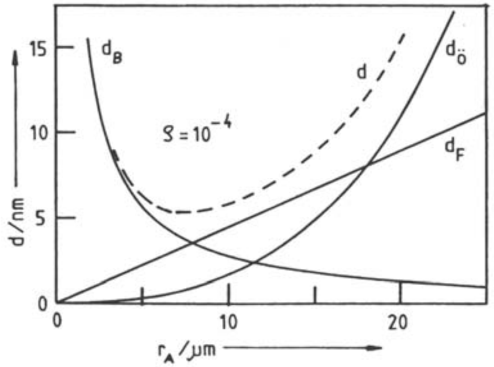

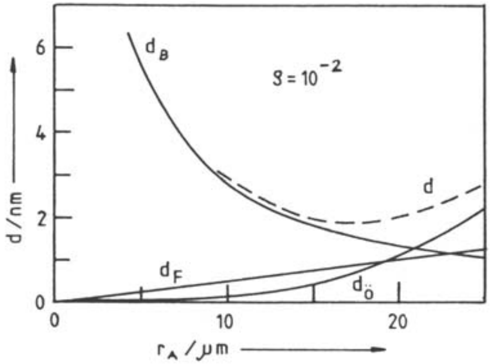

L = 3 mm   E = 25000 eV ΔE_0 = 0.25 eV

Optimum aperture radius

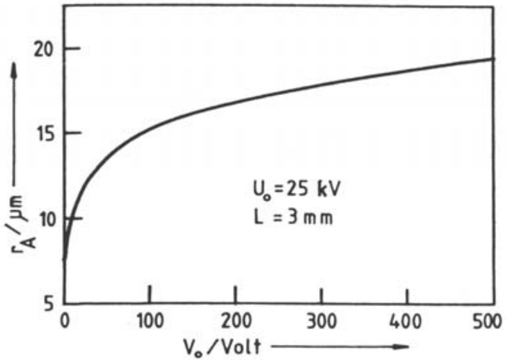

Optimum resolution

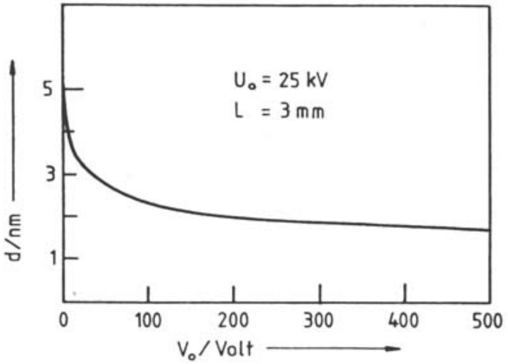

Note: small angle approximation $\sin \alpha \approx \alpha \sim r$

Resolution and optimum aperture

Optimum aperture r_A and resolution-limiting contributions

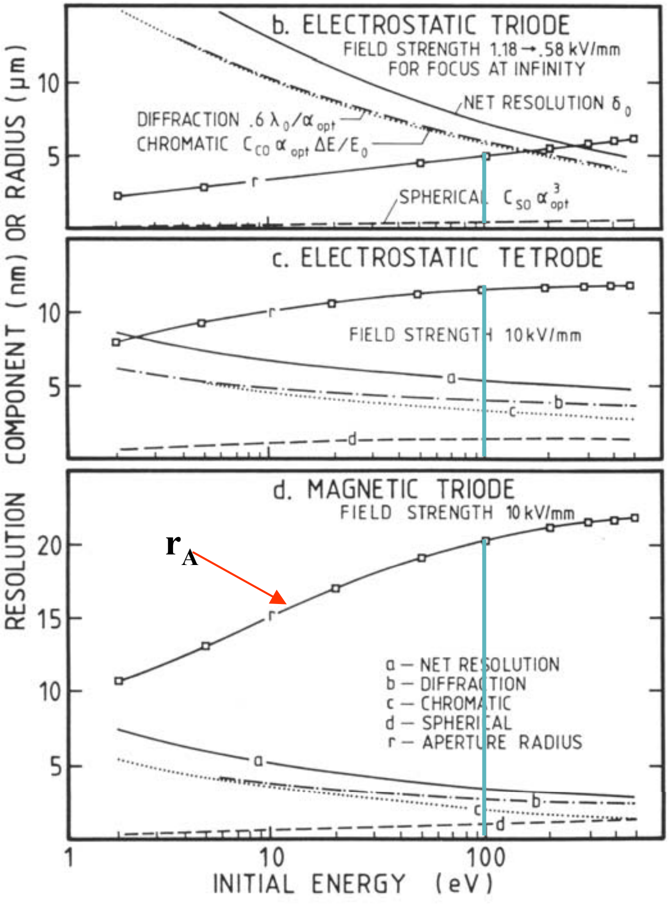

Resolution with optimum aperture
E-dependence at fixed ΔE = 0.5 eV, U_0 = 20 keV

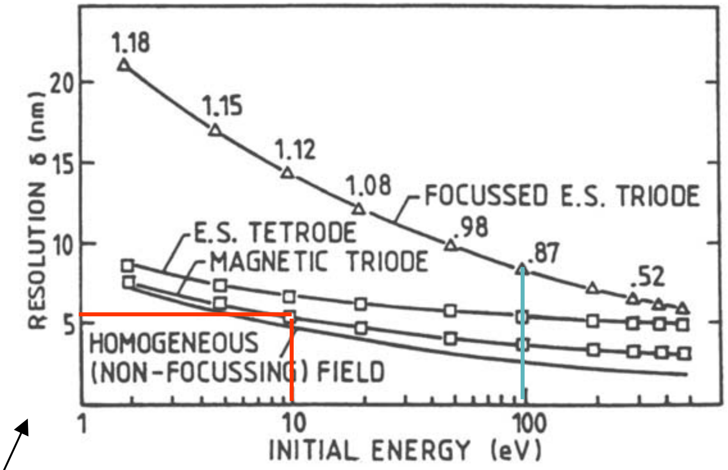

ΔE-dependence at fixed E = 10 eV, U_0 = 18 kV
magnetic triode

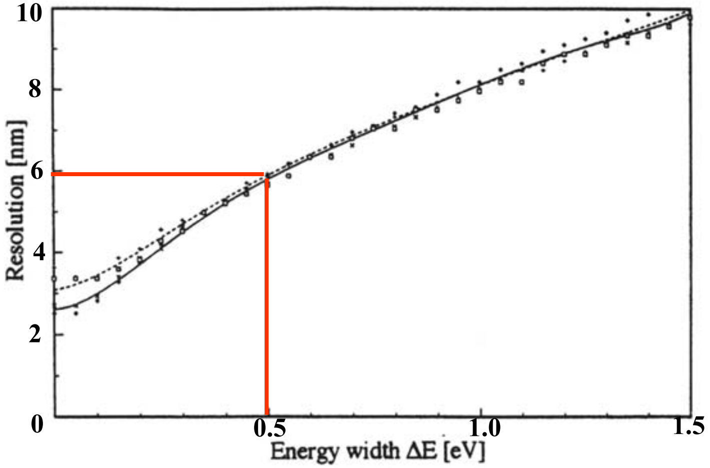

J. Chmelik et al, Optik 83 (1989)155

T. Müller, M.S. thesis, TU Clausthal 1995

Transmission

limited by angle accepted by contrast aperture (r_A)
in back focal plane

Axial distance (in back focal plane) of electron starting at angle α_0

$$r \approx f \sin \alpha_0 \sqrt{E_0/E} \qquad \text{(f focal length)}$$

↓

$$\sin \alpha_0 \approx (r/f) \sqrt{E_0/E}$$

Examples for f = 10 mm, E = 20000eV, r_A =10 μm

E_0	2 eV	200 eV
$\sin \alpha_0$	0.2	0.02
α_0	11.5°	1.15°

In emission microscopy (wide α_0 range) optimum resolution condition

reduces transmission T, therefore

optimize T^n/d^2 instead of $1/d^2$

For cos α distribution $T = \pi \sin^2\alpha_0$

$$T^n/d^2 = \pi \sin^{2n} \alpha_0/d^2$$

Transmission T_n, resolution r_n of homogeneous field

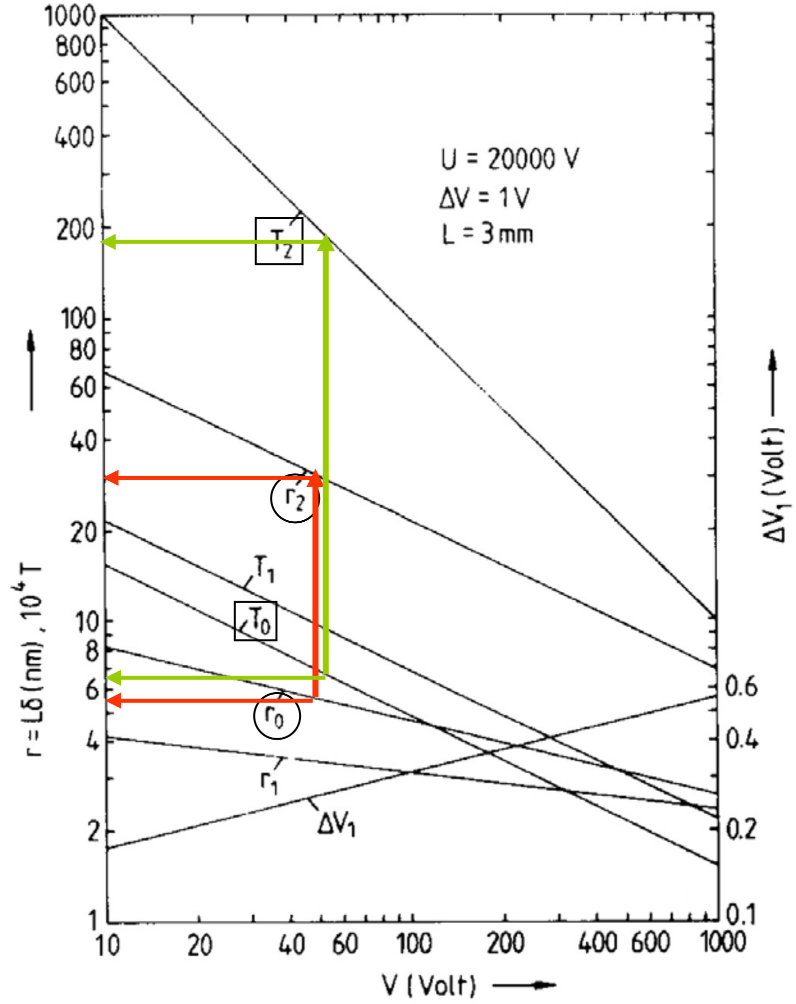

50 eV:
$\Delta T \cong 30$
$\Delta d \cong 5$

E. Bauer, Ultramicroscopy 36 (1991) 52

Photo ionization cross sections

Photon energy selection

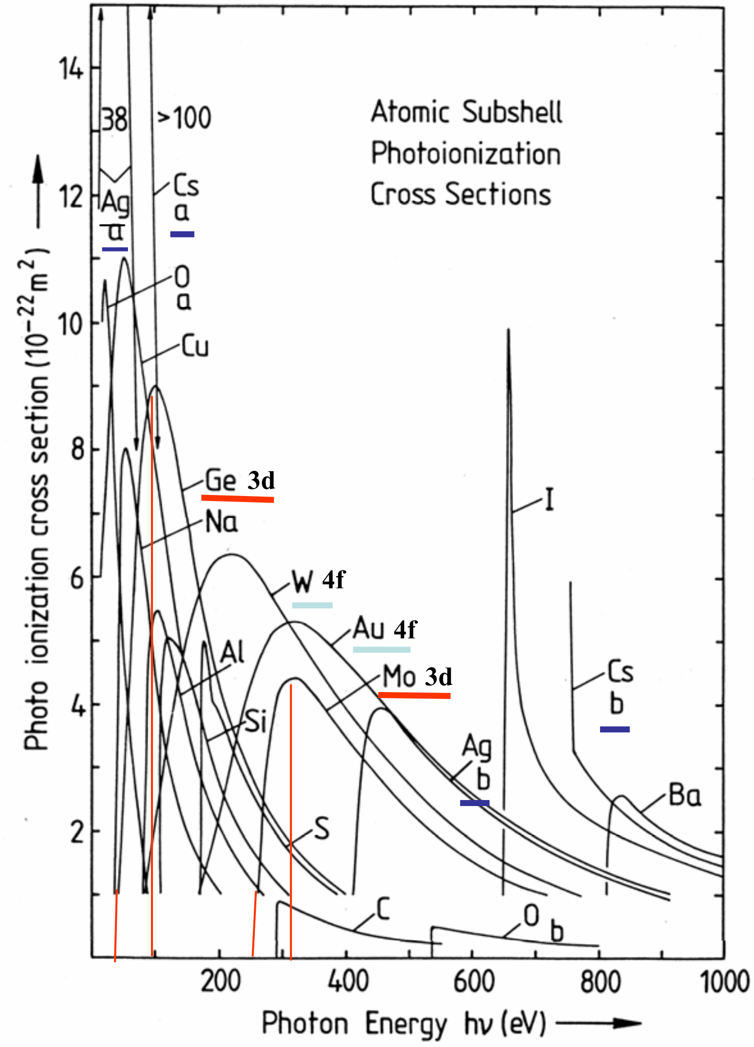

E ≅ 50 – 100 eV

Binding energies (eV)

Ge 3d		**29.8, 29.2**
Mo 3d		**231.1, 227.9**
W 4f		**33.6, 31.4**
Au 4f		**87.6, 84.0**
Ag		
a	**4d**	**≈ 5**
b	**3d**	**374.0, 368.3**
Cs		
a	**4d**	**79.8, 77.5**
b	**3d**	**740.5, 726.6**

J.J. Yeh and I. Lindau,
Atomic Data 1985

Aberration correction in electron optics

Round **convex** lenses

electrostatic mirror

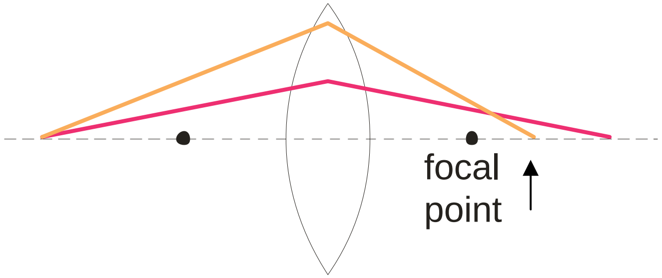

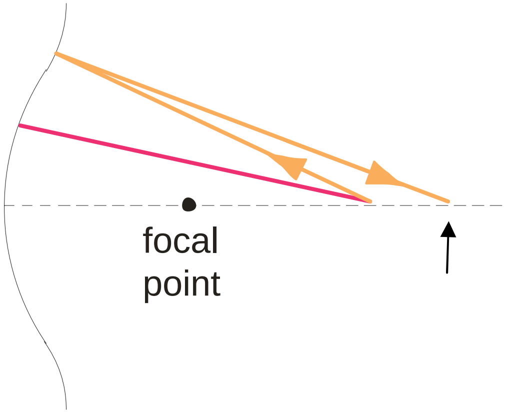

Spherical aberration

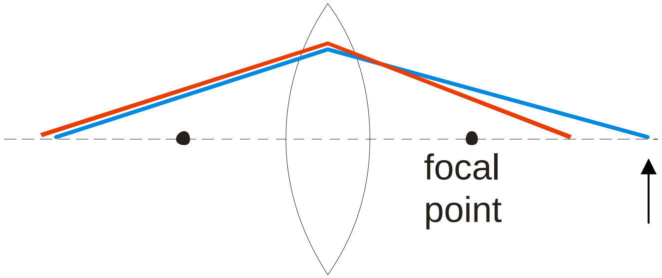

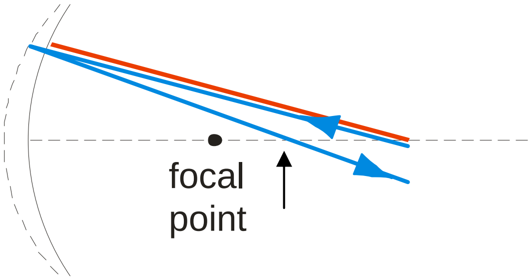

Chromatic aberration

Equipotential surfaces
in a diode mirror

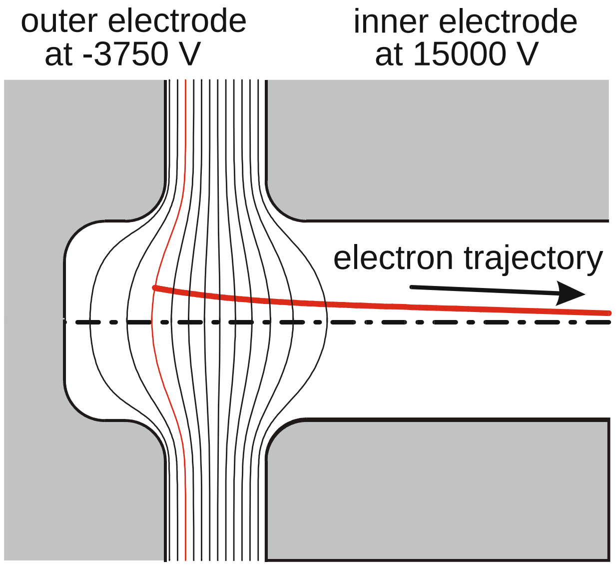

Resolution and transmission improvement with aberration correction

Example: SMART

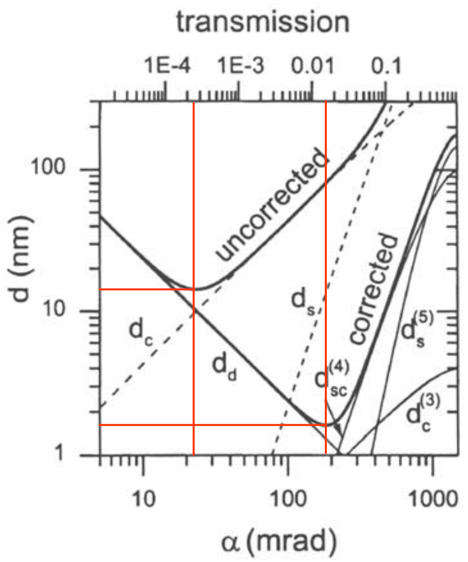

E_0 = 10 eV, ΔE = 2 eV, F = 5 kV/mm

Δd ≅ 1/5, ΔT ≅ 600

ΔE (eV)		
0.1	□	■
1.0	○	●
5.0	△	▲
	without	with
	correction	

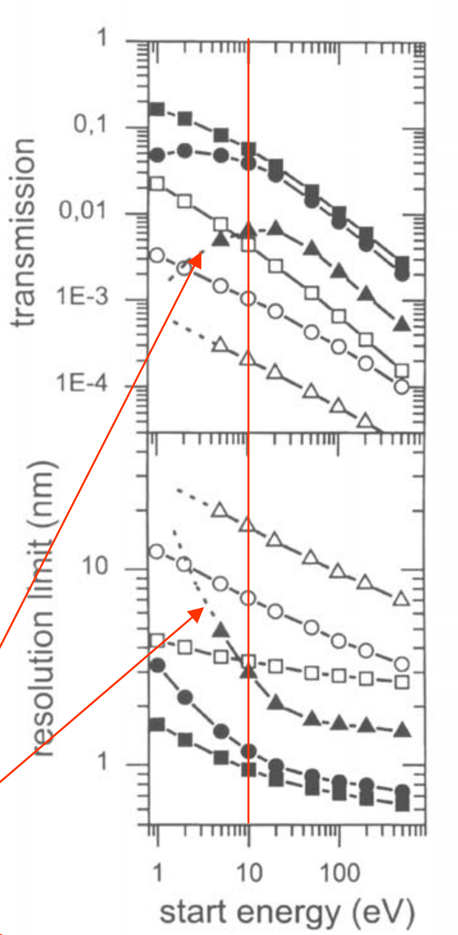

Energy filter needed for secondary electrons

Calculations: D. Preikszas
From Th. Schmidt et al,
Surf. Rev. Lett. 9 (2002) 223

Basic PEEM schematic

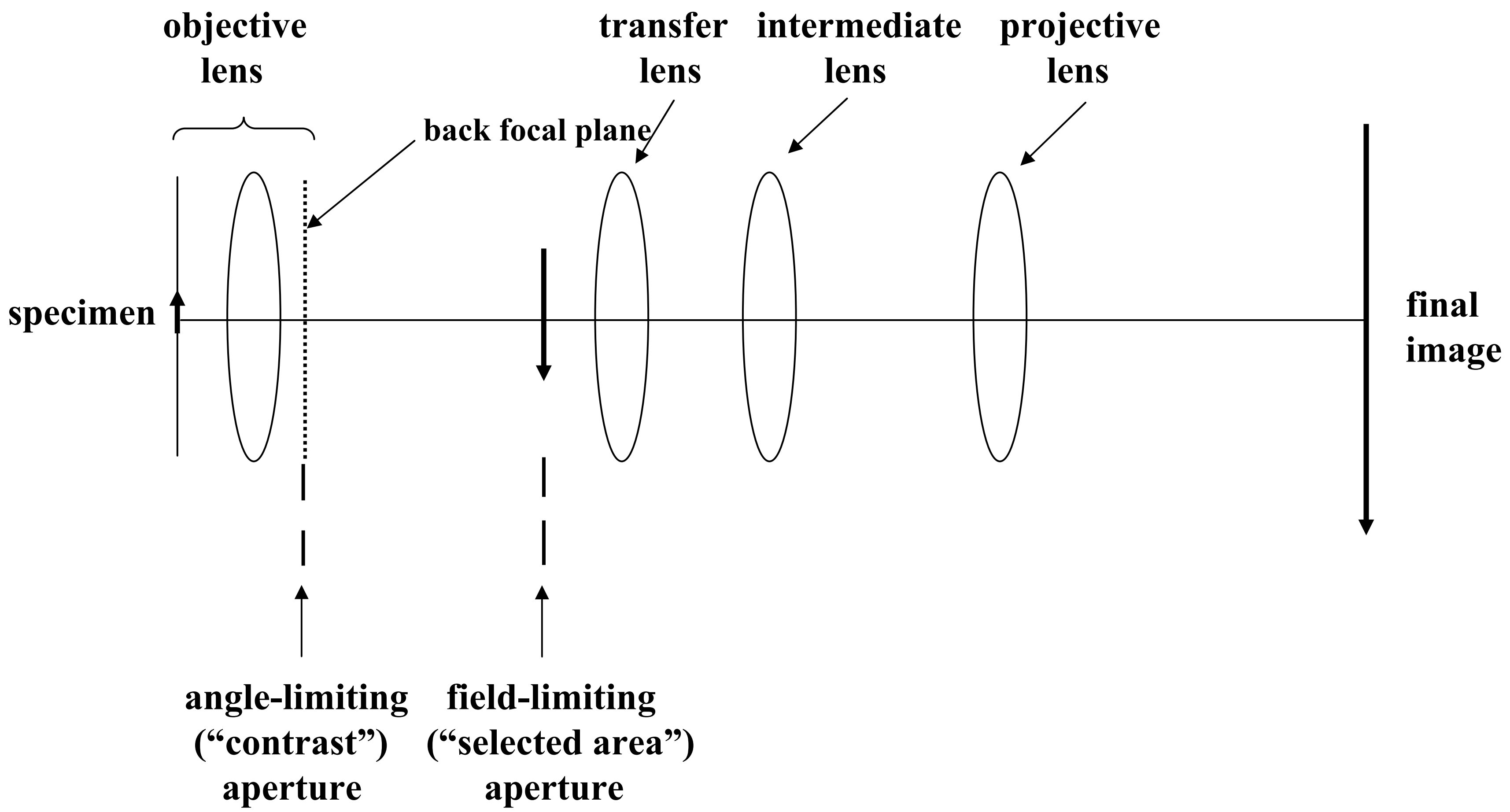
objective lens

back focal plane

transfer lens

intermediate lens

projective lens

specimen

final image

angle-limiting (“contrast”) aperture

field-limiting (“selected area”) aperture

Electrostatic PEEM examples

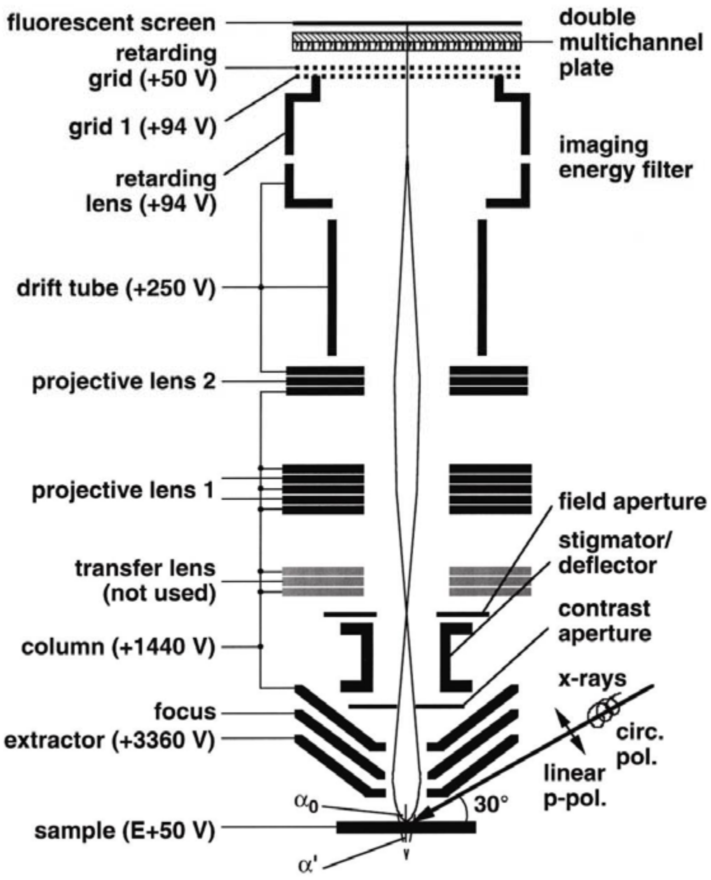

Focus PEEM
with high pass filter

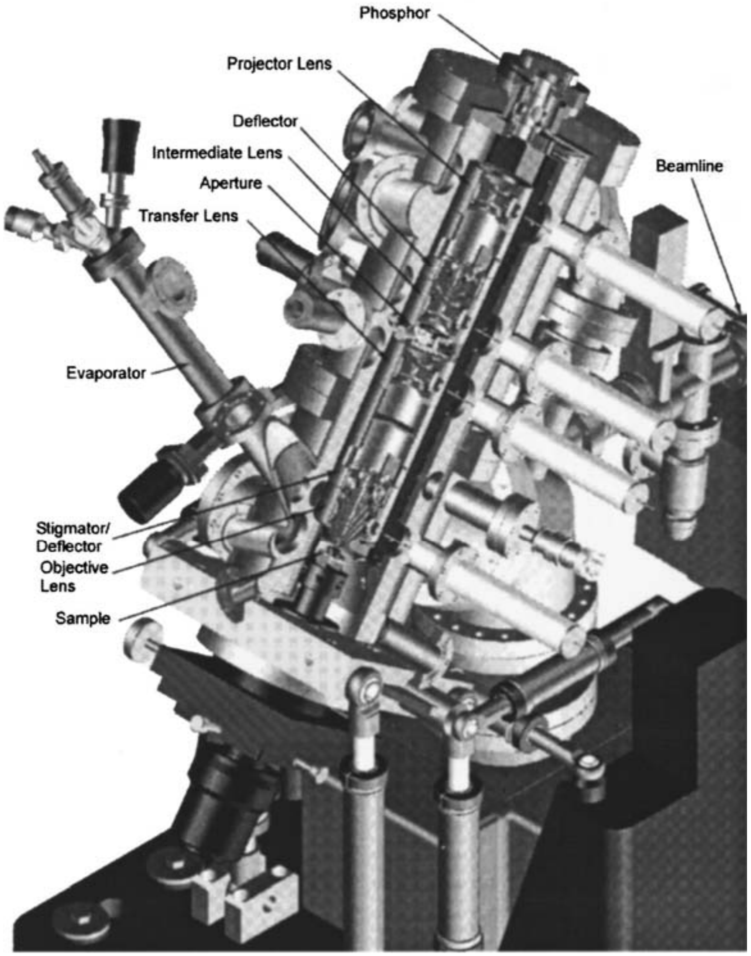

ALS PEEM II

Magnetic PEEM (ELMITEC)

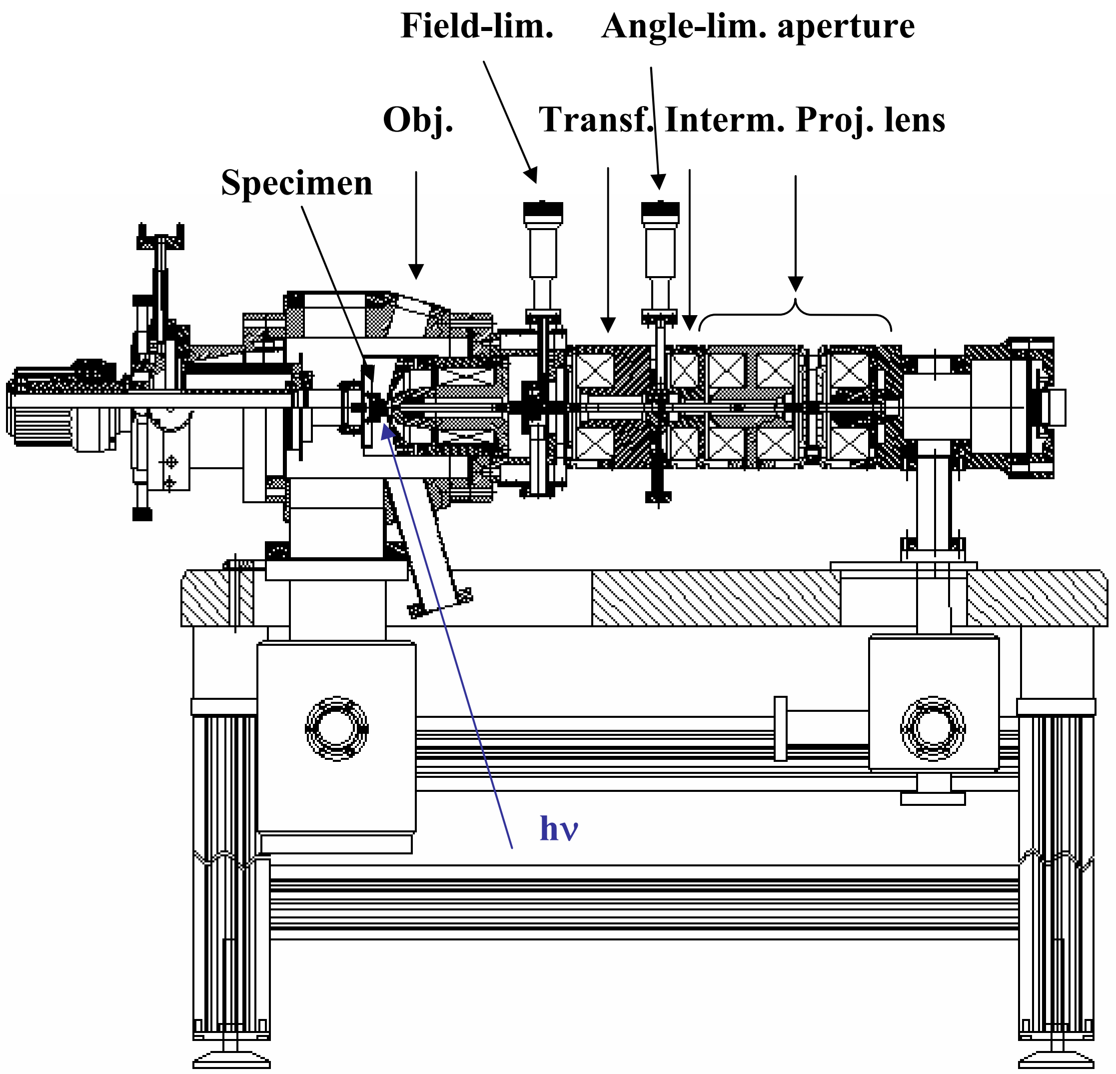

Field-lim.

Angle-lim. aperture

Obj.

Transf. Interm. Proj. lens

Specimen

hν

Spectroscopic PEEM with band pass filter

ELMITEC

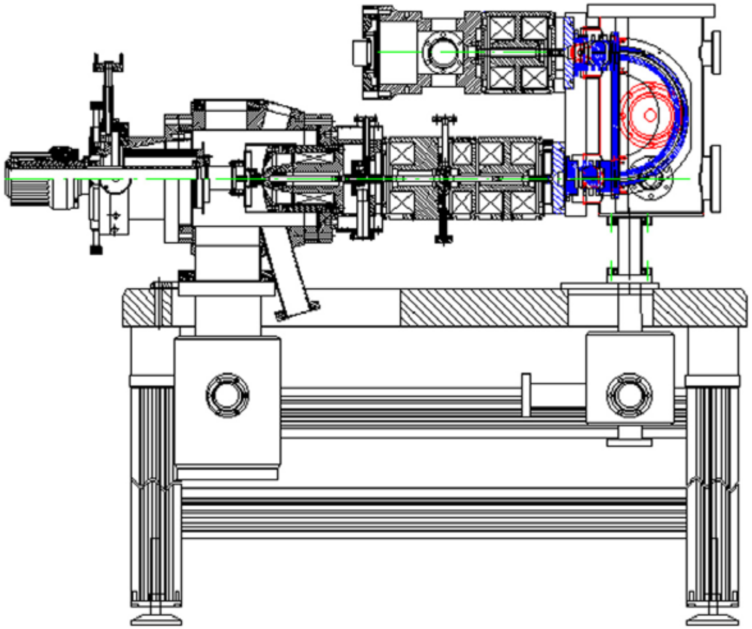

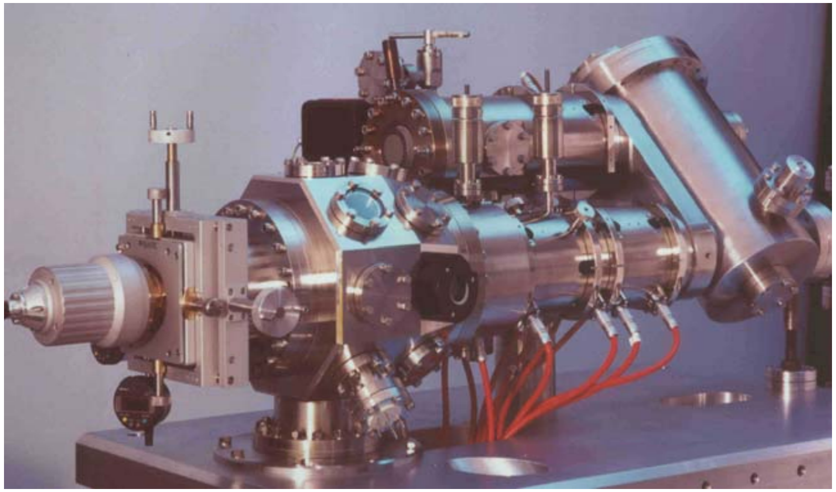

Contrast mechanisms

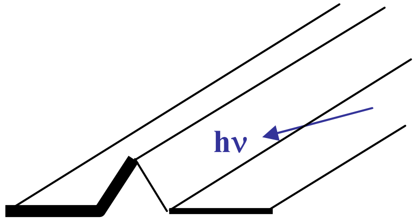

1 Topographic contrast due to oblique illumination and field distortion

2 Work function contrast at low E_0 (escape probability!)

3 Chemical contrast due to inner shell ionization

4 Magnetic contrast via XMCD and XMLD

No structural contrast, therefore combination with
Low Energy Electron Microscopy
(LEEM)

The usefulness of LEEM

Properties not visible with PEEM, but with LEEM

atomic steps

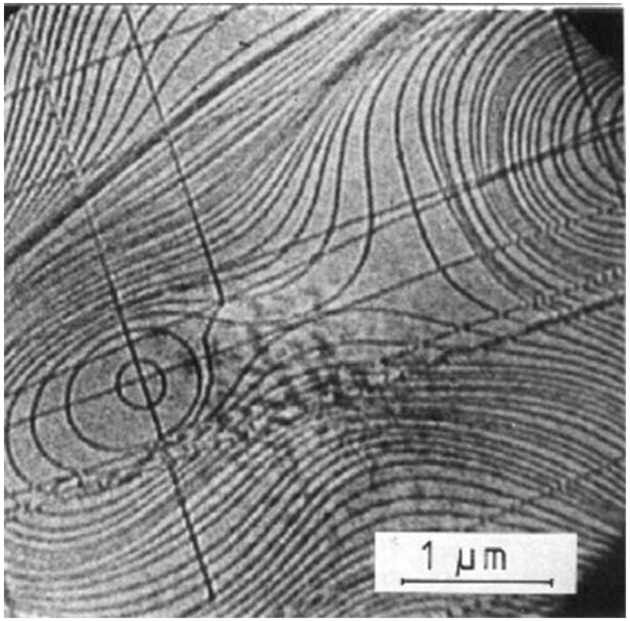

Mo(110)

Interference contrast

domain orientations

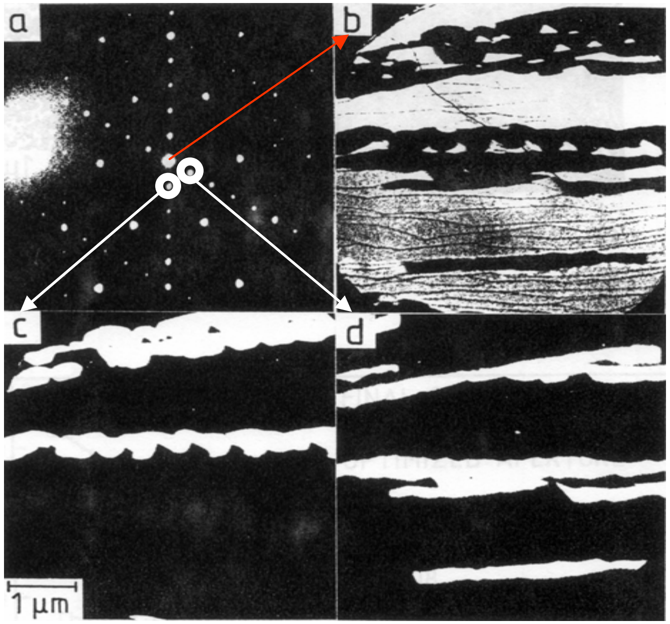

Au(√3×√3)-R30° + Au(5 ×2) on Si(111)
b c,d

Diffraction contrast

LEEM also much brighter and better resolution ⇒ use for focusing in XPEEM

LEED much easier to interpret than PED ⇒ use for structure analysis

Basic LEEM schematic

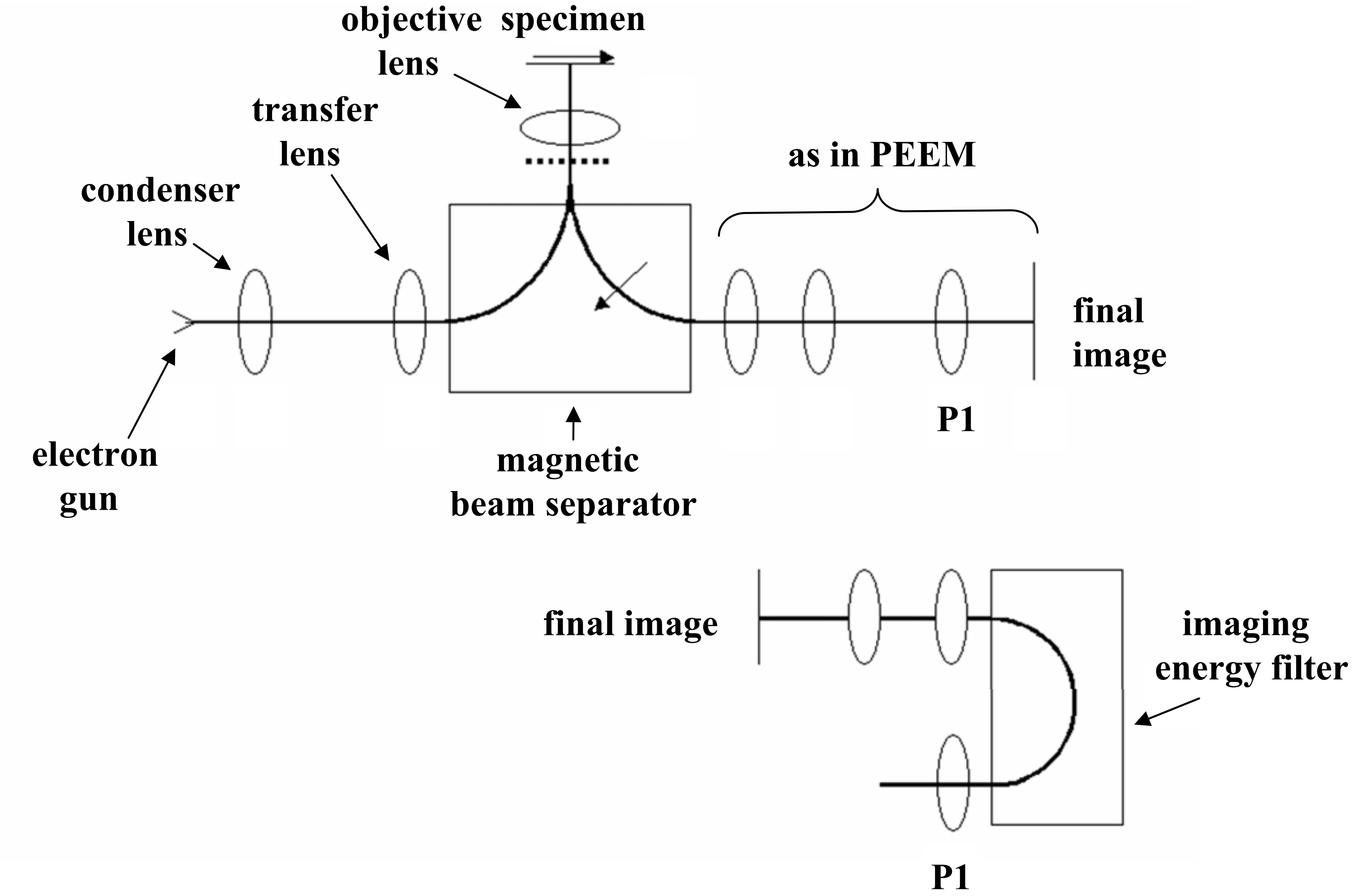

Spectroscopic Photo Emission and Low Energy Electron Microscope

SPELEEM

ELMITEC

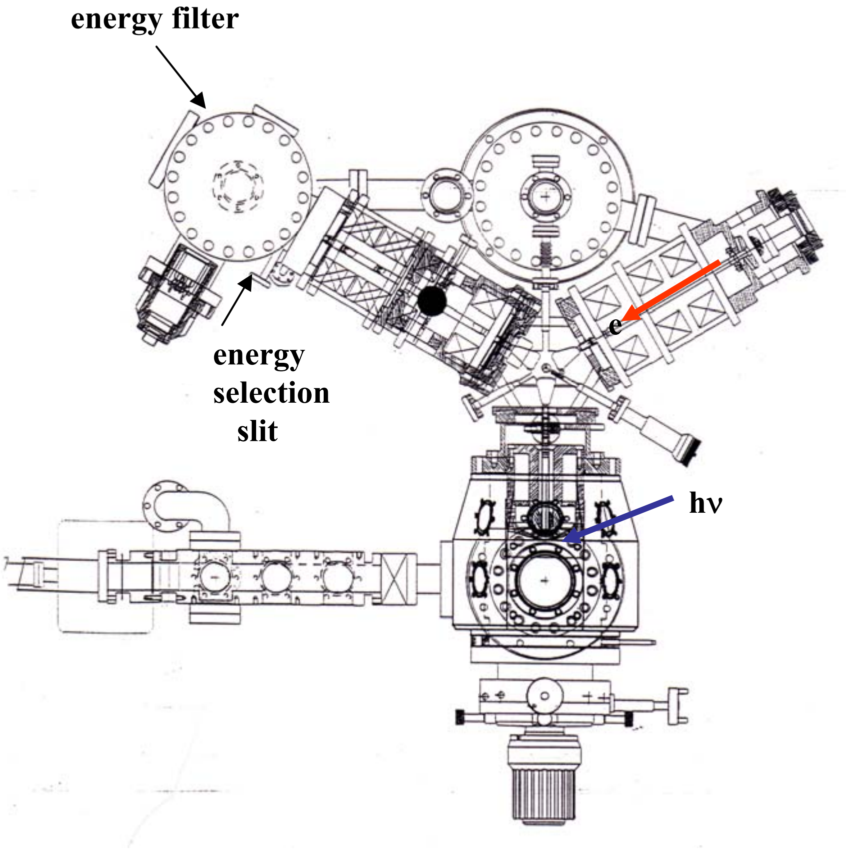

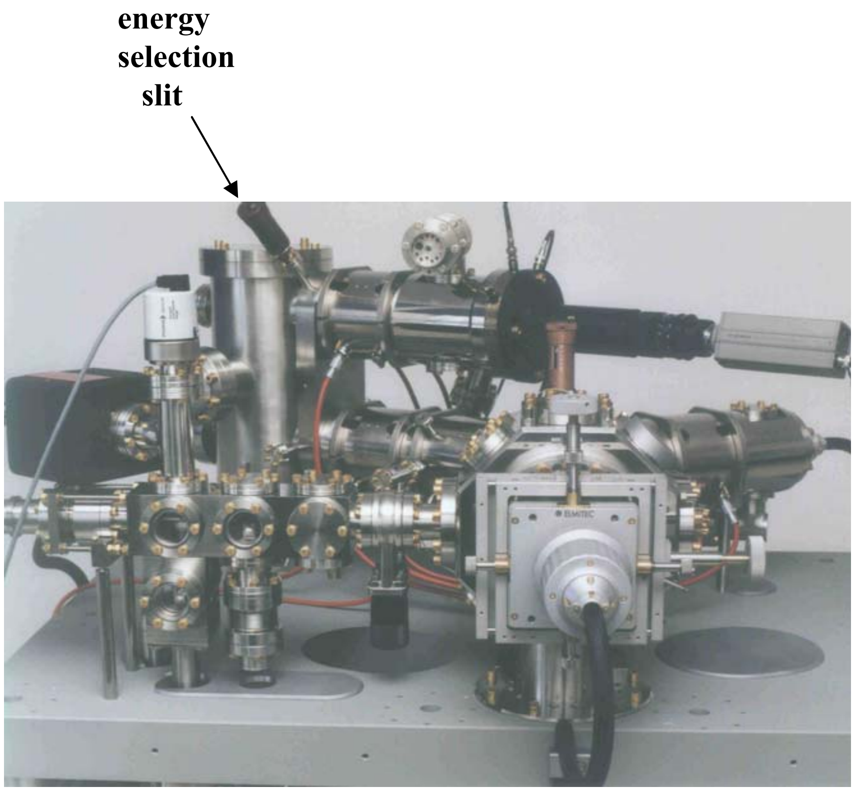

SPELEEM side view

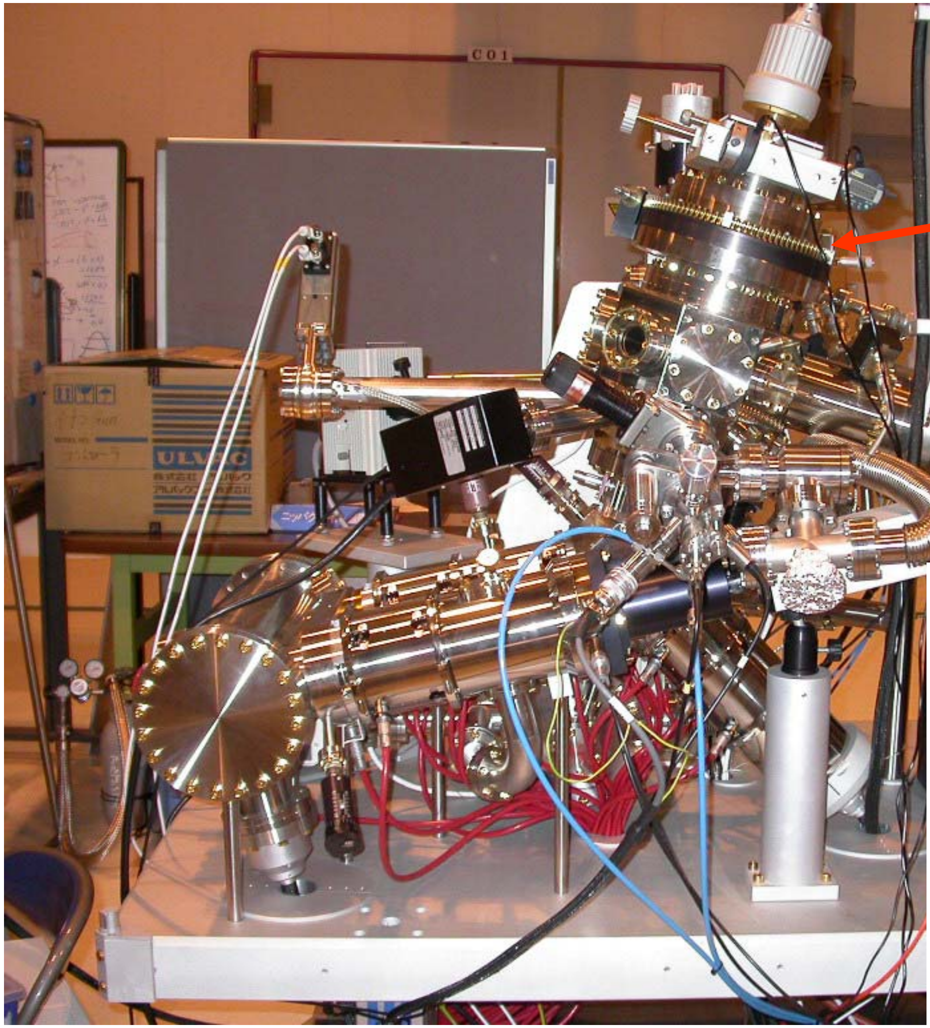

Differentially Pumped Rotary Platform

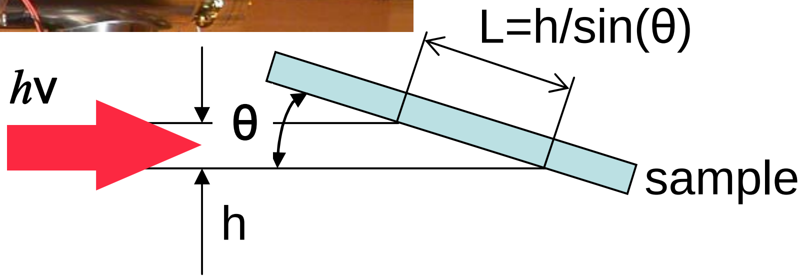

L≈3.6h (Θ=16 º)

h: vertical size of *h*ν

θ: inclination angle

L: effective irradiation width

SPring8

Aberration-corrected SPELEEM

SMART (BESSY II)

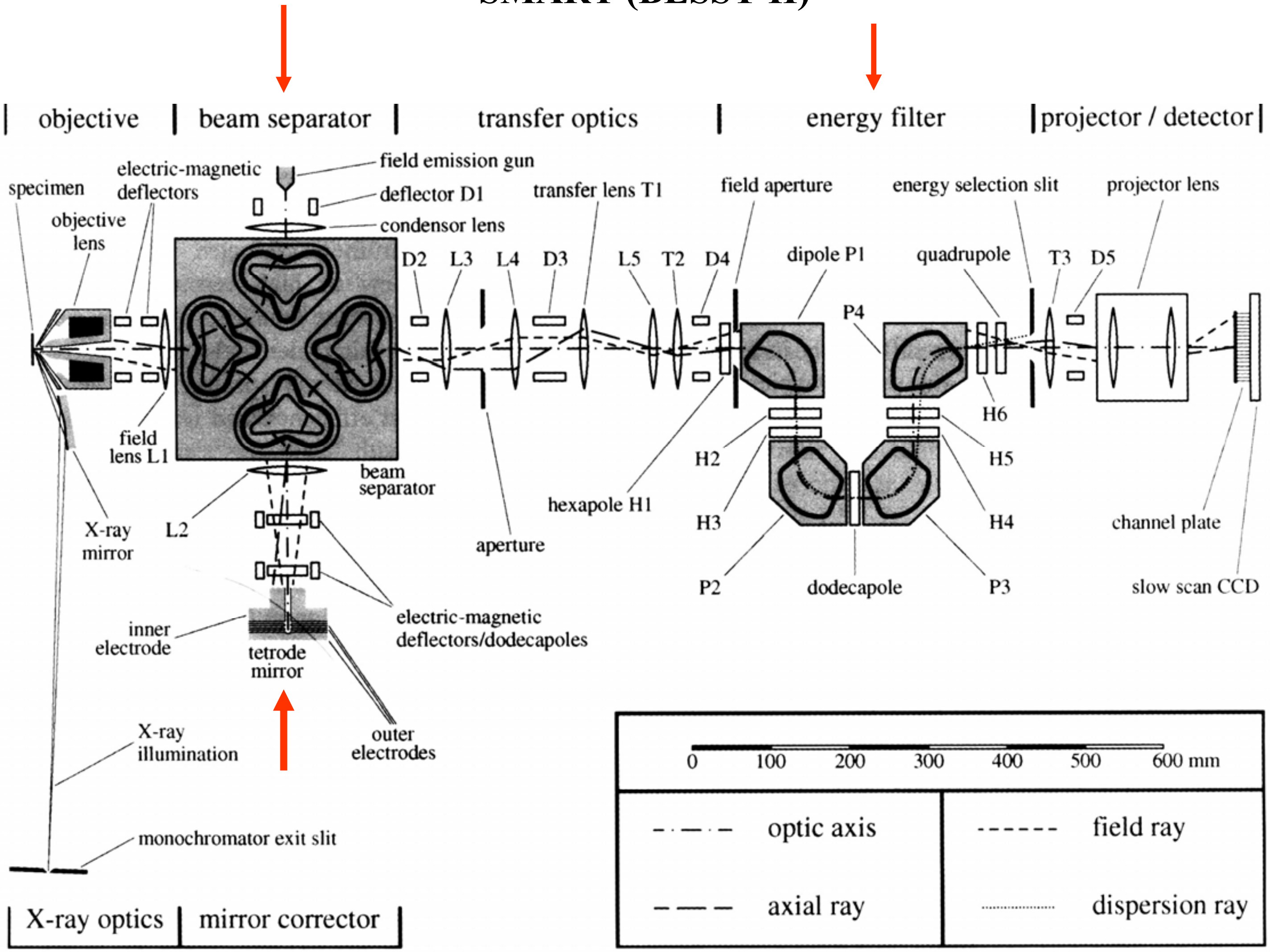

H. Rose, D. Preikszas, Nucl. Instr. & Meth. A363, 201 (1995)

SMART top view

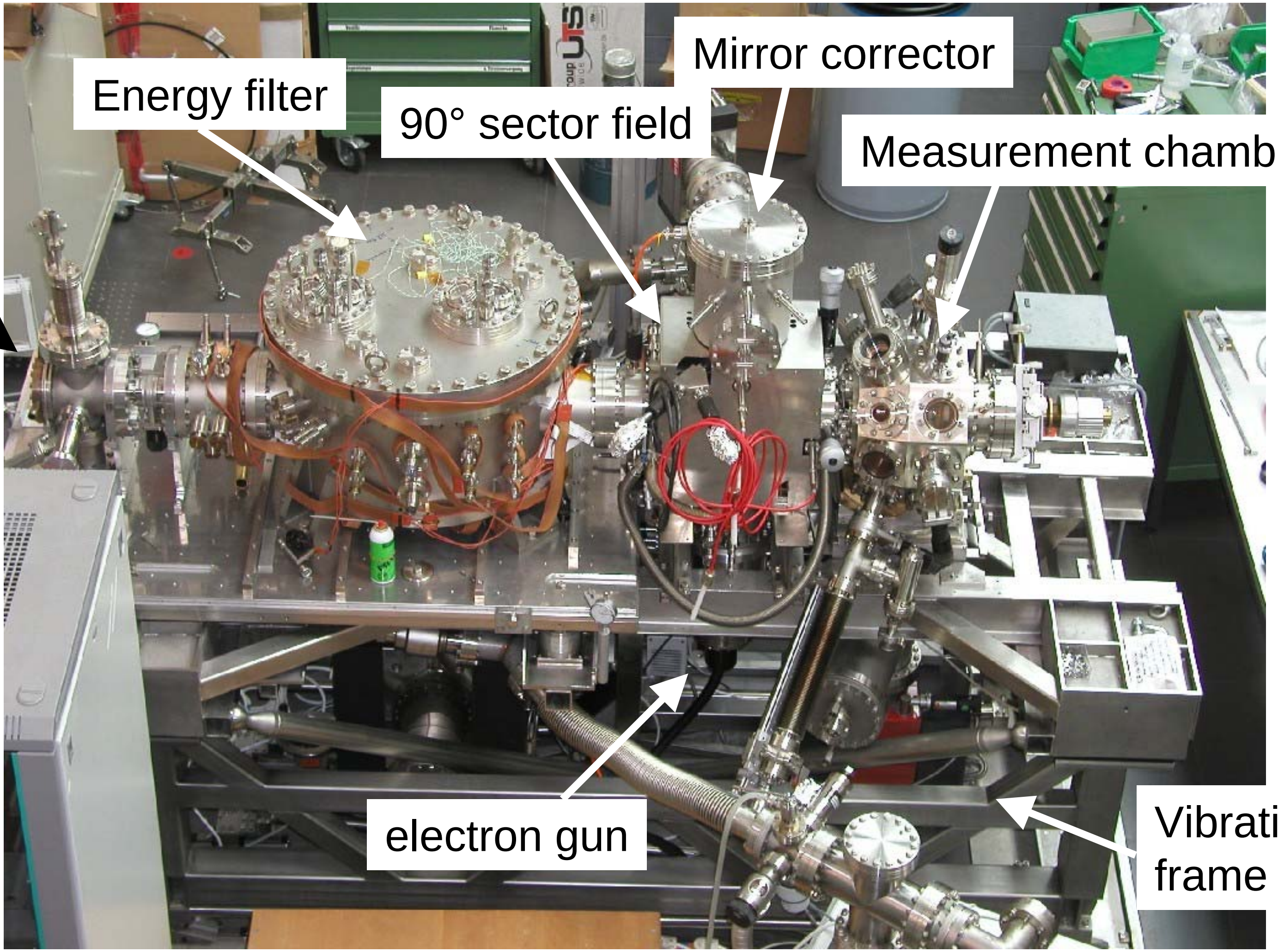

Detector

Energy filter

90° sector field

Mirror corrector

Measurement chamber

electron gun

Vibration damped frame

Th. Schmidt April 2004

Operation modes of a SPELEEM

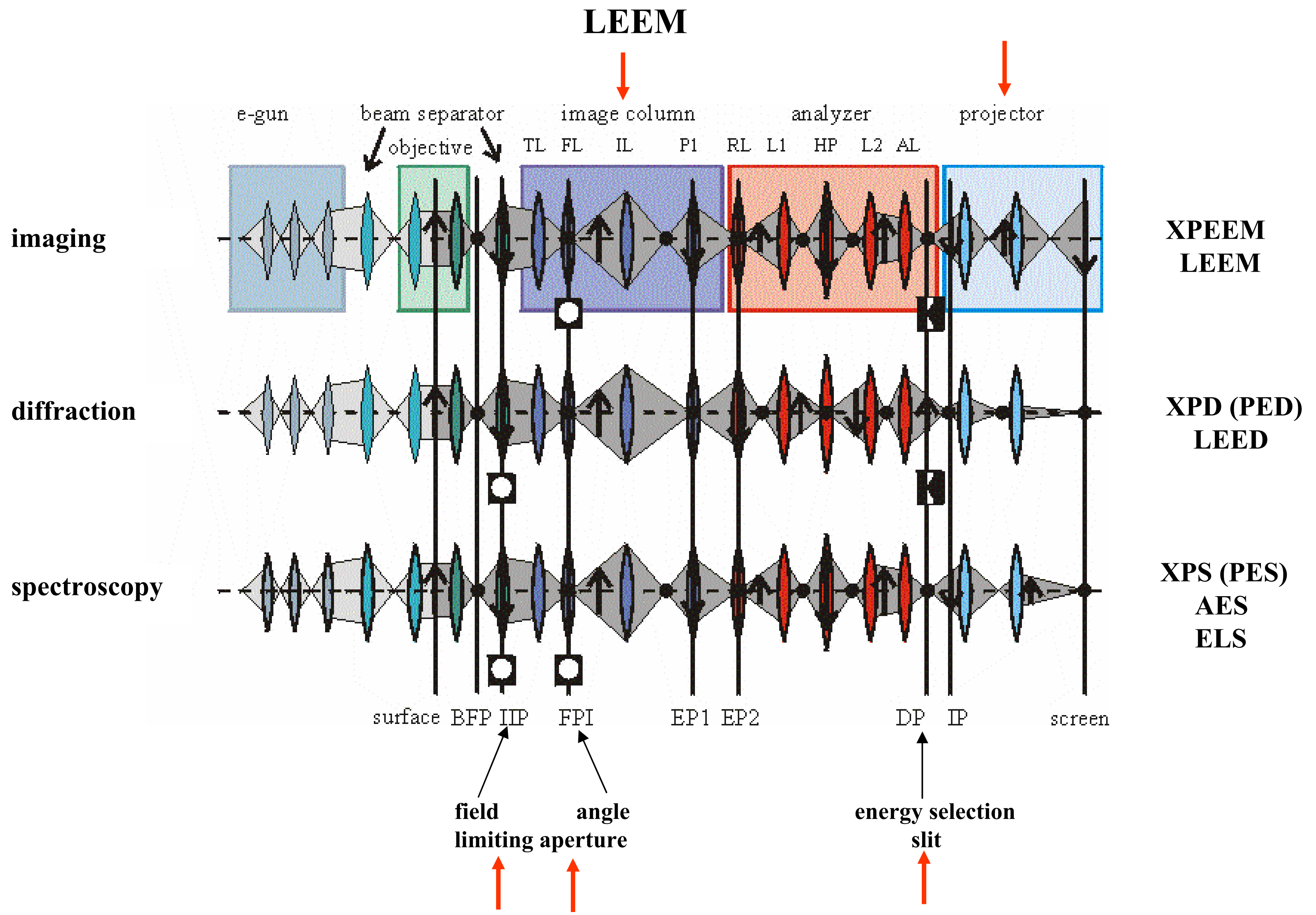

Th. Schmidt et al, Surf. Rev. Lett. 5 (1998) 1287

Operation modes of a SPELEEM

PEEM

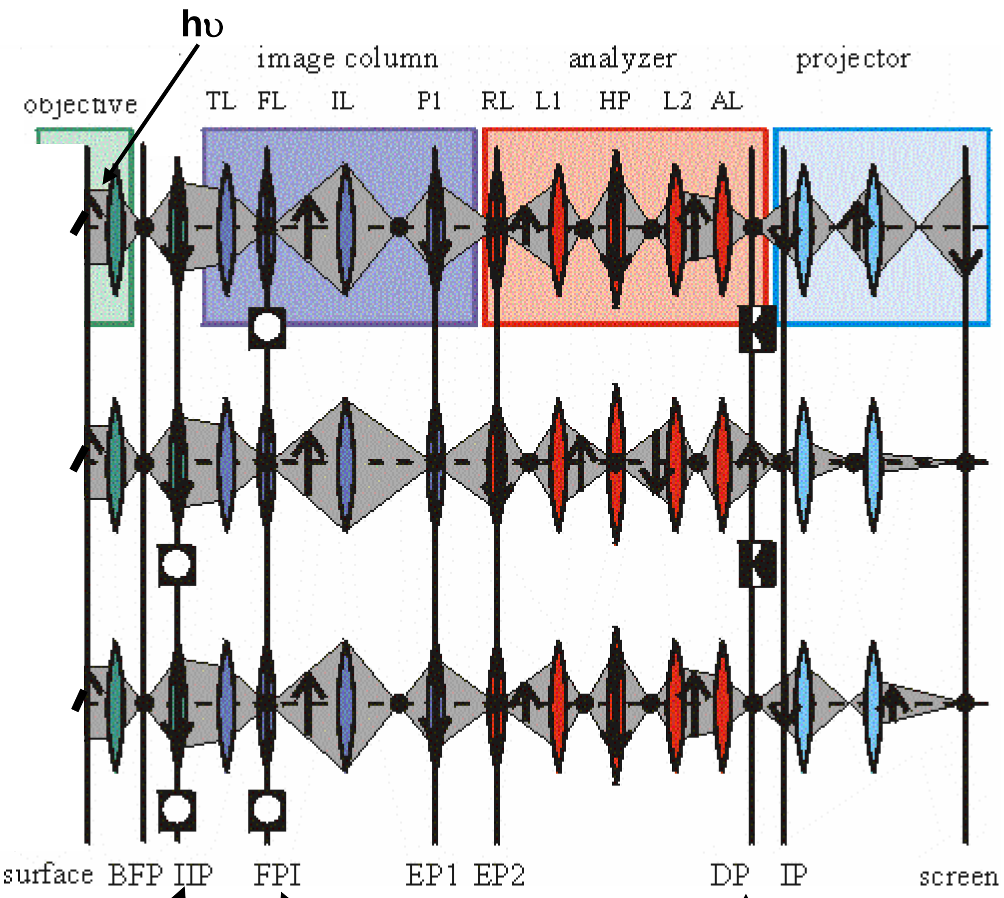

imaging

diffraction

spectroscopy

XPEEM

XPD (PED)

XPS (PES)
AES

field
limiting aperture

angle

energy selection
slit

Th. Schmidt et al, Surf. Rev. Lett. 5 (1998) 1287

Operation modes of a SPELEEM

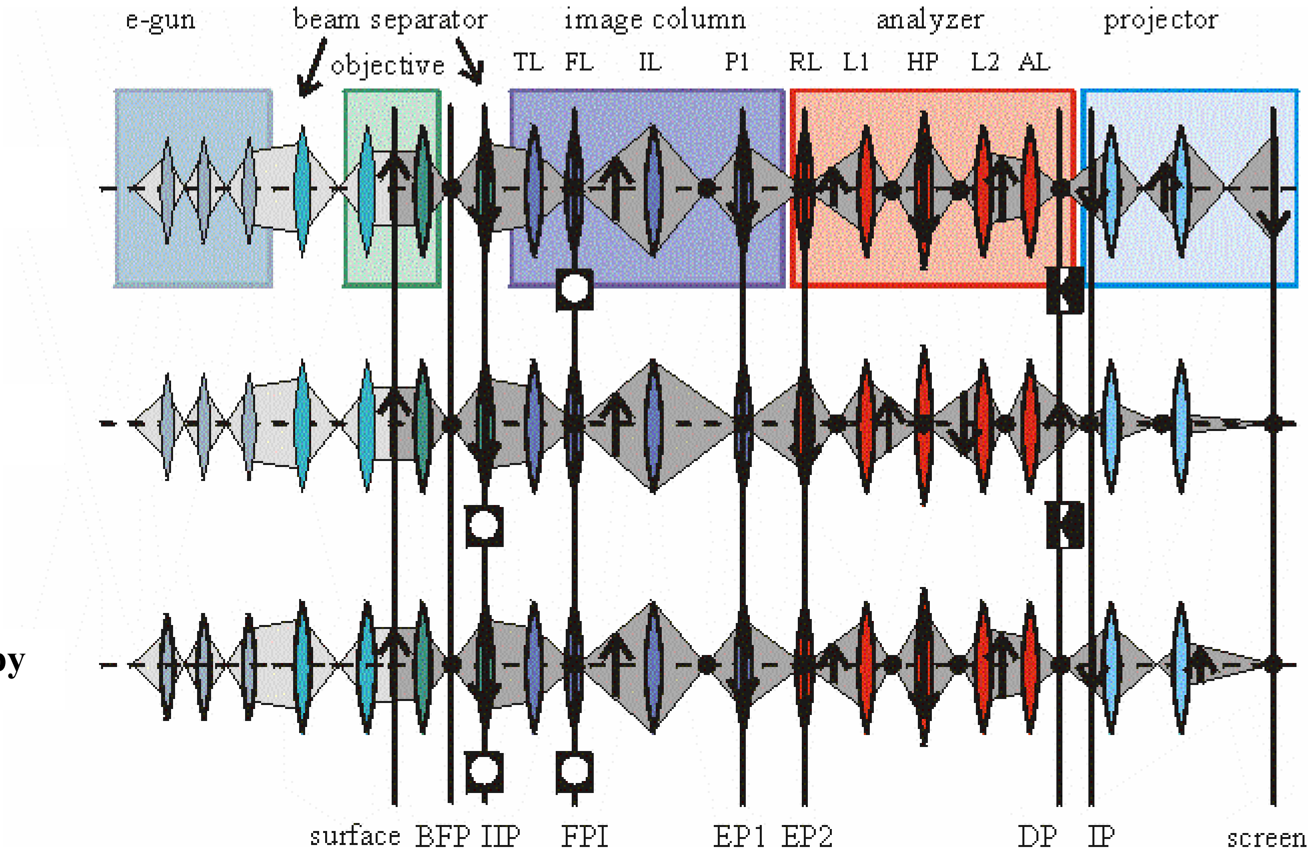

imaging

mode 1

XPEEM

LEEM

diffraction

XPD (PED)

LEED

spectroscopy

XPS (PES)

AES

ELS

field **angle**

limiting aperture

energy selection slit

Image plane

Th. Schmidt et al, Surf. Rev. Lett. 5 (1998) 1287

Chemical imaging (mode 1)

secondary electrons
spatial resolution
$\sigma_{Ag4d} \approx 5\ \sigma_{W5d}$
$h\nu = 65$ eV >> $E_i < 10$ eV
$\Delta E_F \leq 1$ eV

photo electrons
energy resolution
$h\nu = 65$ eV, images in 0.2 eV steps
10-60 sec/image 0.25 μm^2 areas
$\Delta E_F \leq 0.5$ eV, $\Delta E_{chem} \approx 0.15$ eV

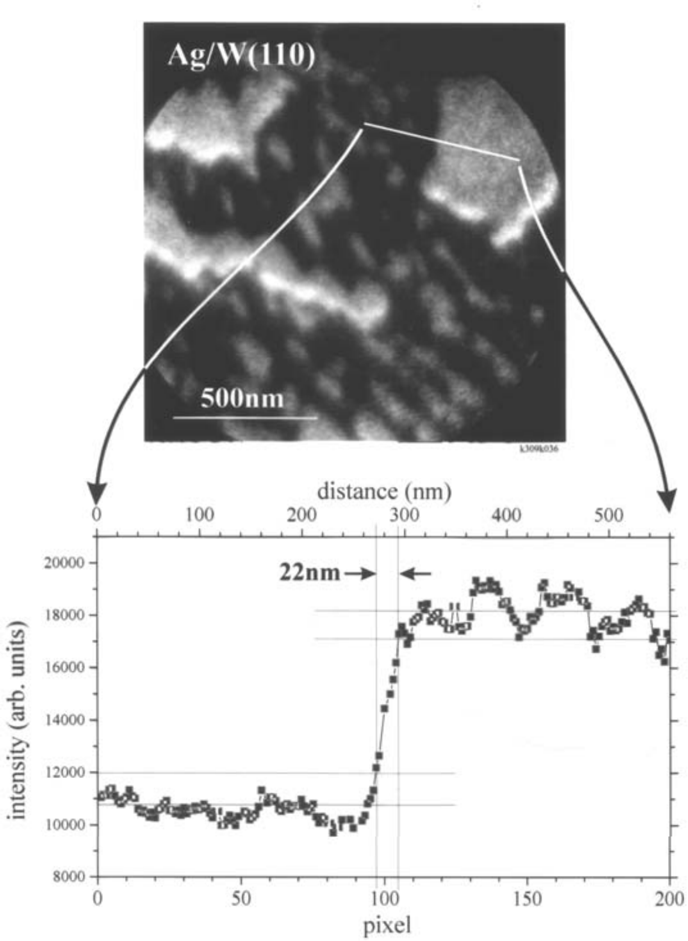

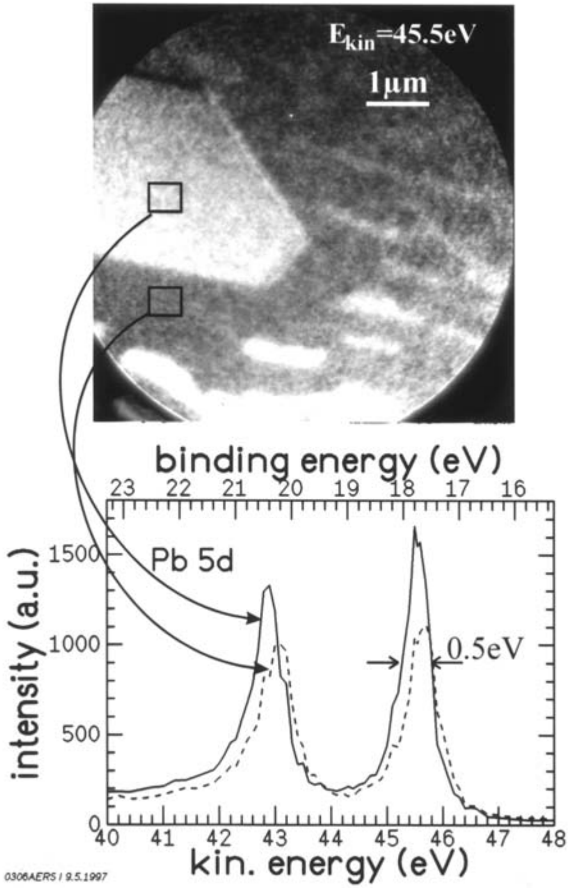

Pb/W(110)

Th. Schmidt et al, Surf. Rev. Lett. 5 (1998) 1287

Operation modes of a SPELEEM

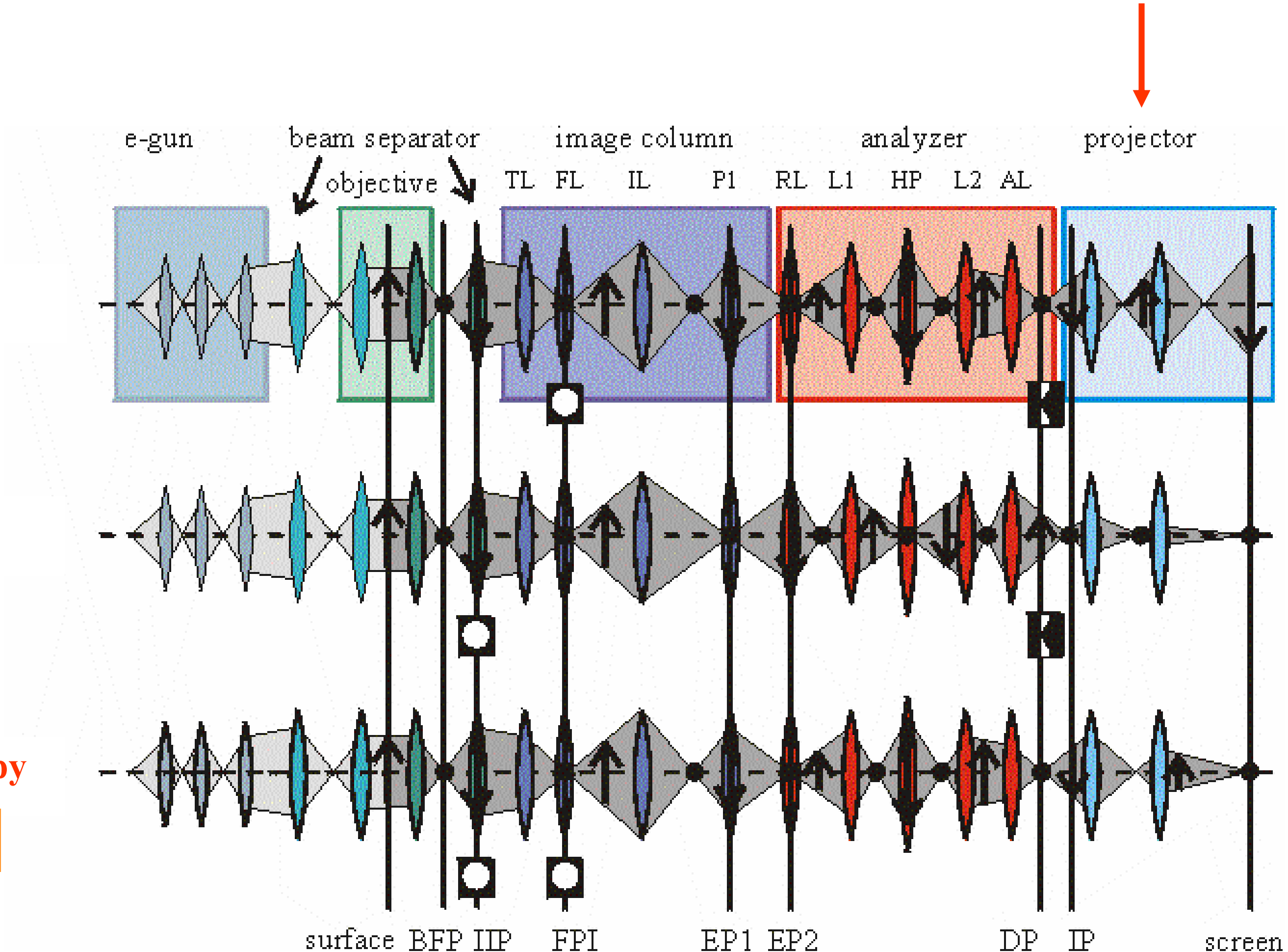

imaging

XPEEM
LEEM

diffraction

XPD (PED)
LEED

spectroscopy

mode 3

XPS (PES)
AES
ELS

field limiting aperture

angle limiting aperture

energy selection slit

Dispersive plane

Th. Schmidt et al, Surf. Rev. Lett. 5 (1998) 1287

Fast local spectroscopy
by imaging the dispersive plane (mode 3)

$\alpha = 8^o$ (contrast aperture), $0.8 \mu m^2$ area (selected field aperture)
20 eV full dispersion, 60 sec
$h\nu = 48$ eV

8 monolayers Pb on Si(111)-$\sqrt{3}\times\sqrt{3}$-Ag

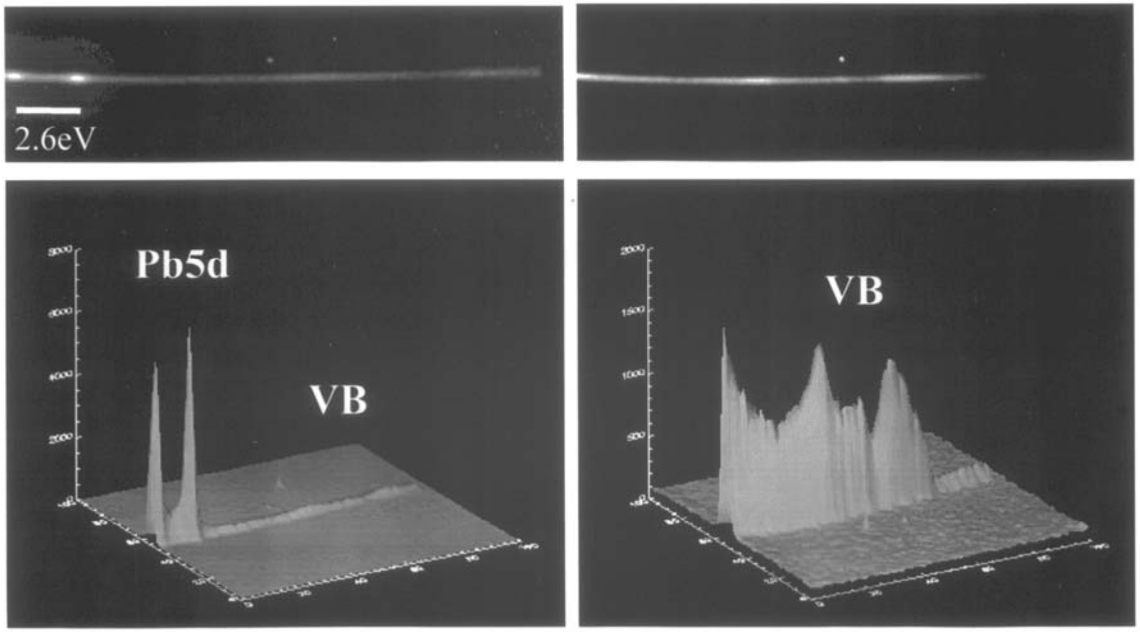

Dispersive plane

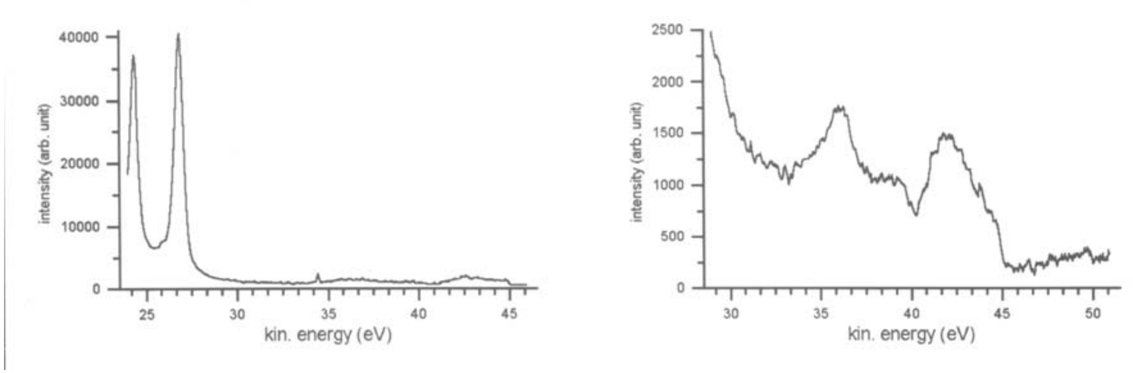

Th. Schmidt et al, Surf. Rev. Lett. 5 (1998) 1287

Surface sensitivity of photo electrons

versus secondary electrons

valence band region

hν = 48 eV

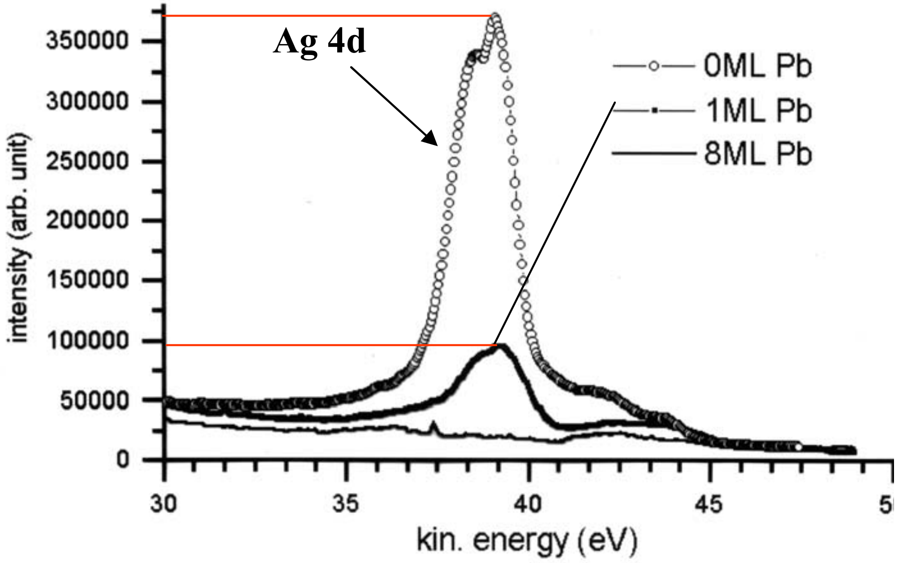

Pb on Si(111) – Ag (√3×√3) – R30°
(1 monolayer Ag)

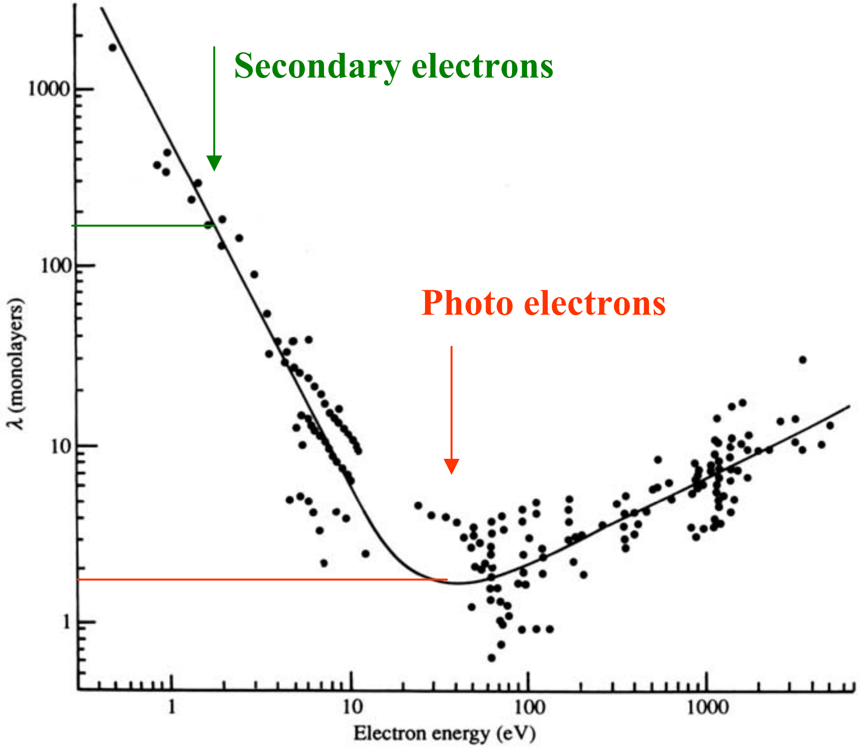

Inelastic mean free path
("universal curve")
determines sampling depth

Th. Schmidt et al, 1998

Operation modes of a SPELEEM

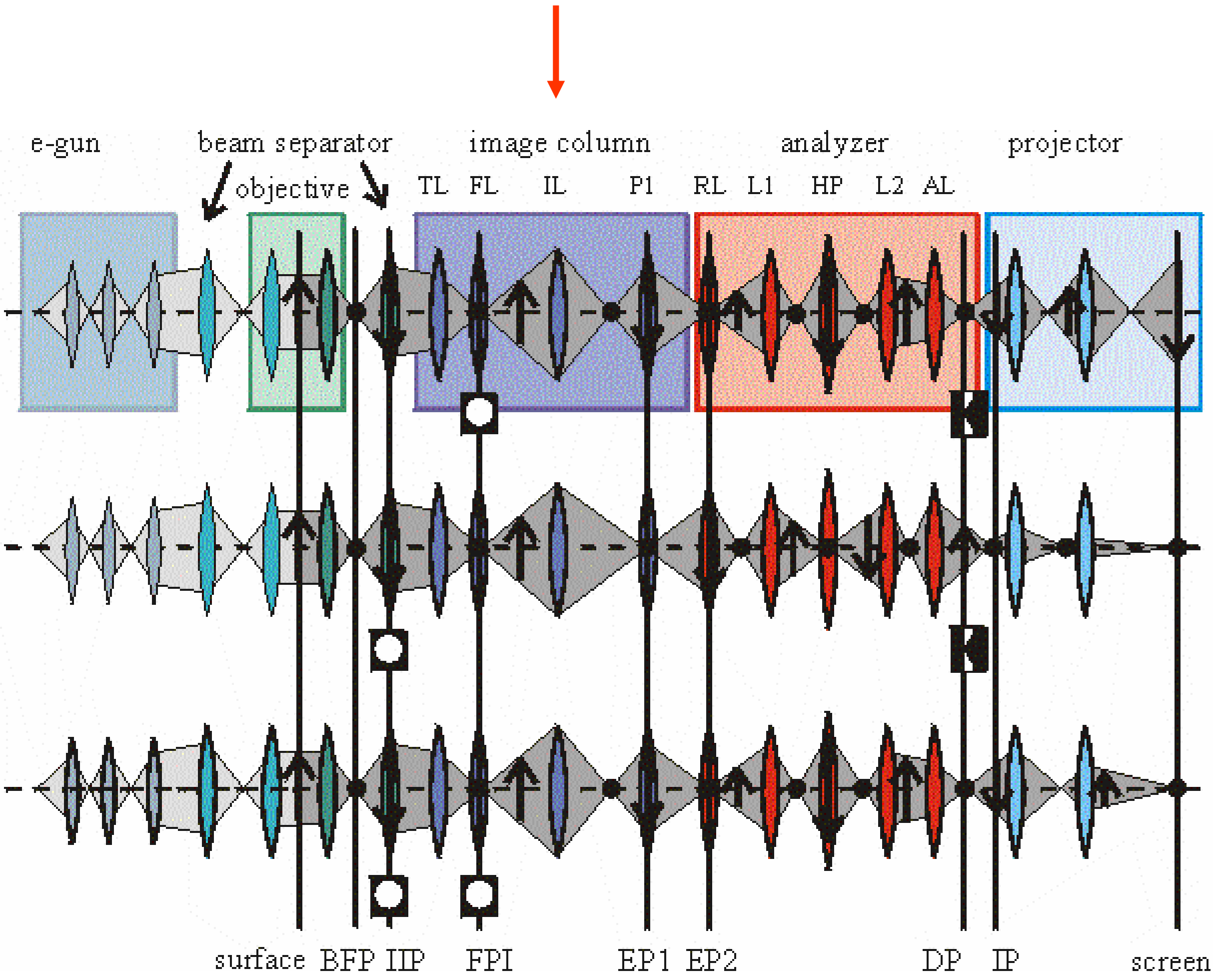

imaging

XPEEM
LEEM

diffraction

mode 2

XPD (PED)
LEED

spectroscopy

XPS (PES)
AES
ELS

field **angle**
limiting aperture

energy selection
slit

Image plane

Th. Schmidt et al, Surf. Rev. Lett. 5 (1998) 1287

Local photo electron diffraction (mode 2)

Pb 5d photo electrons

from 0.8 μm² area (selected field aperture)

E_{kin} 23.0 eV 28.0 eV 33.0 eV 38.0 eV

$5d_{3/2}$

$5d_{5/2}$

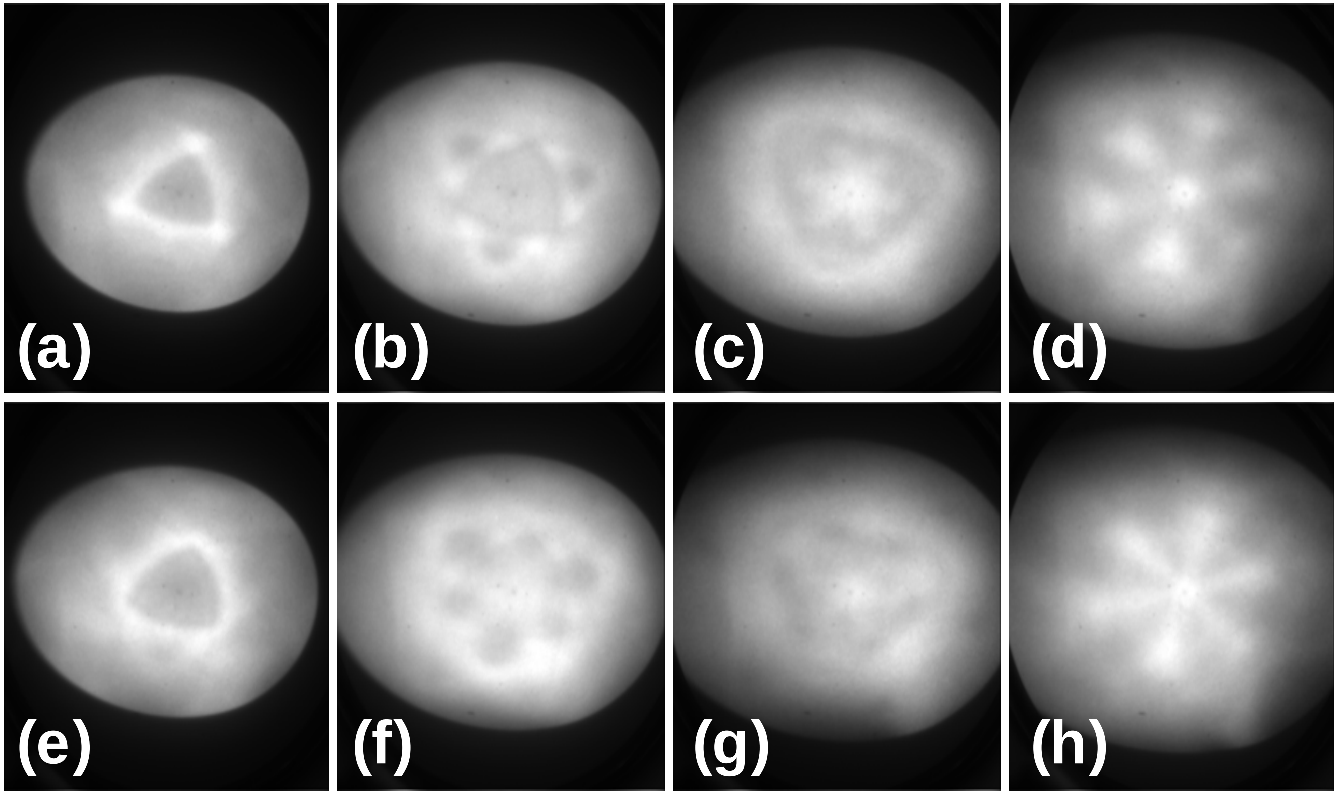

E_{kin} 25.6 eV 30.6 eV 35.6 eV 40.6 eV

hν 43.5 eV 48.5 eV 53.5 eV 58.5 eV

Th. Schmidt et al, Surf. Rev. Lett. 5 (1998) 1287

Simultaneously acquired PED and LEED pattern

Pb 5d 38 eV

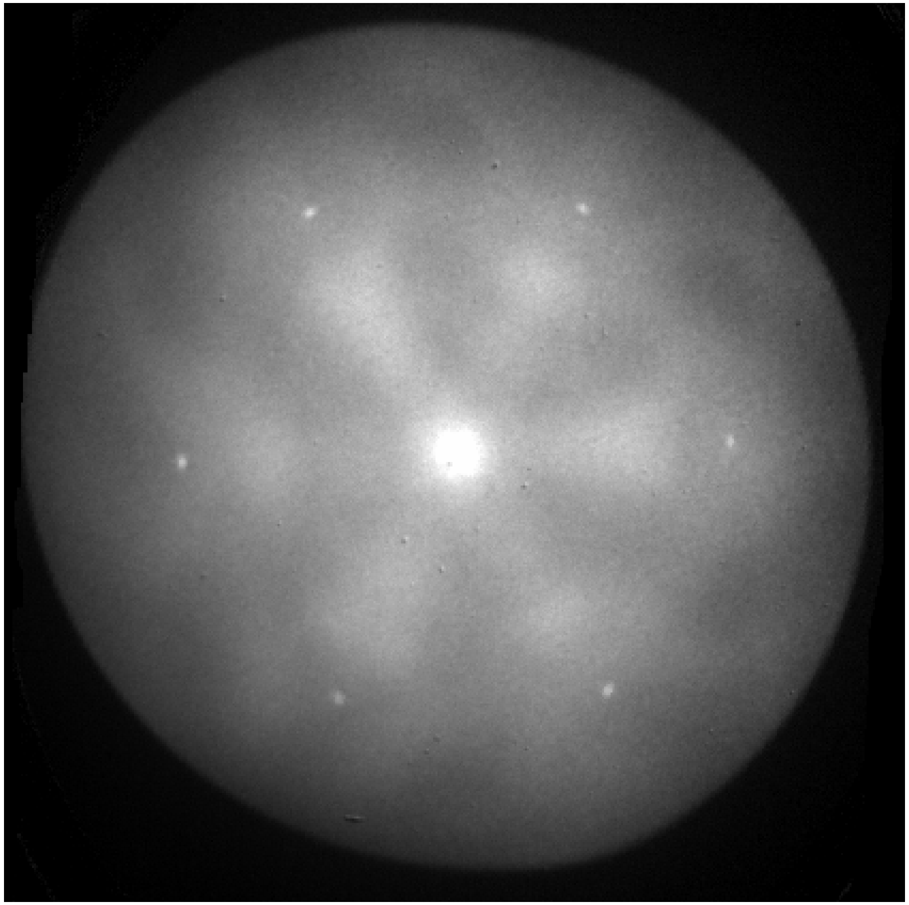

Local band structure analysis (mode 2)

Conduction band of Pb(111)

5 Pb monolayers on Si(111) – Au √3×√3 – R30°

hν = 73 eV, 0.8 μm² area (selected field aperture)

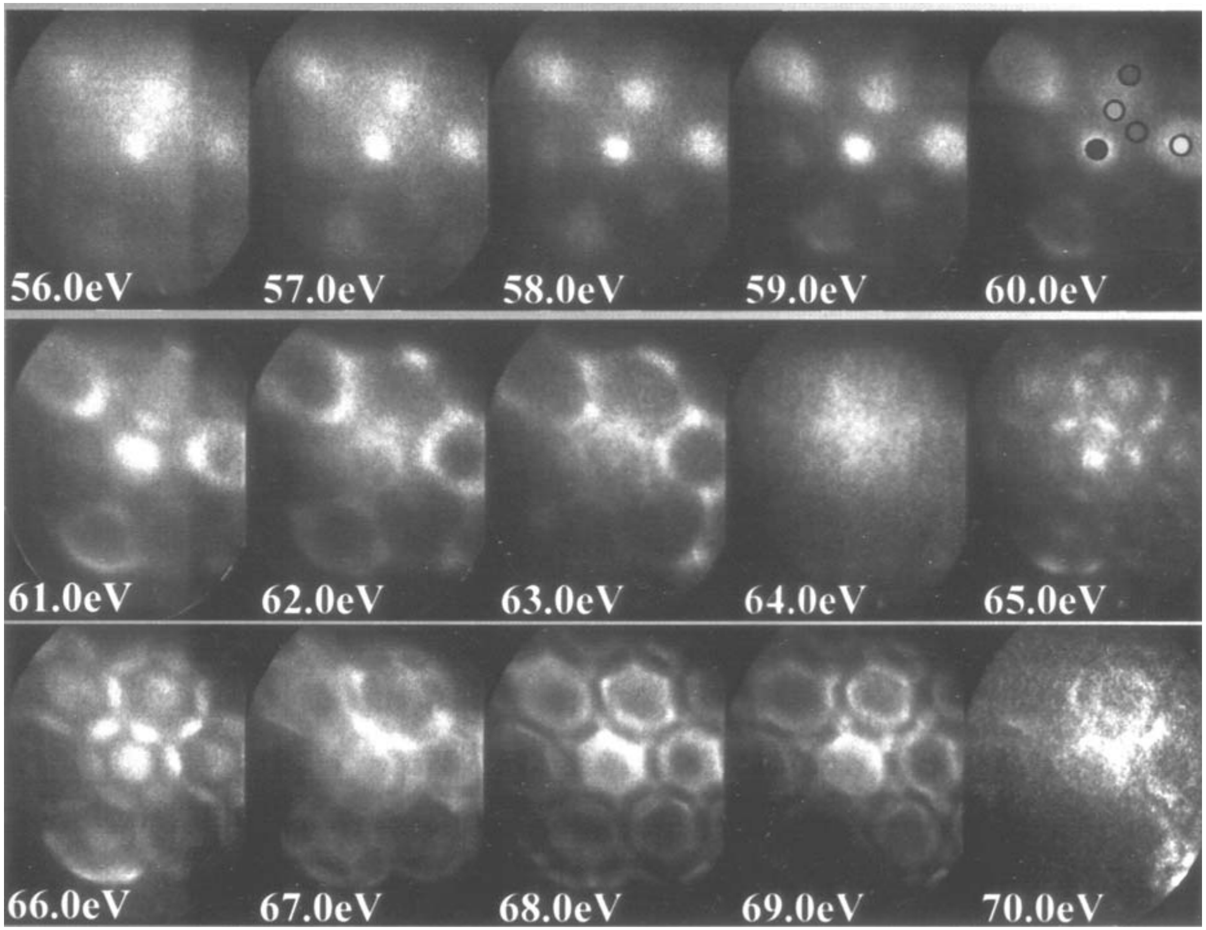

Parameter: E_{kin}

Th. Schmidt, 1997

Magnetic imaging

XMCD, (XMLD)

↓

ALS

Domain structures in 20 nm thick Co films

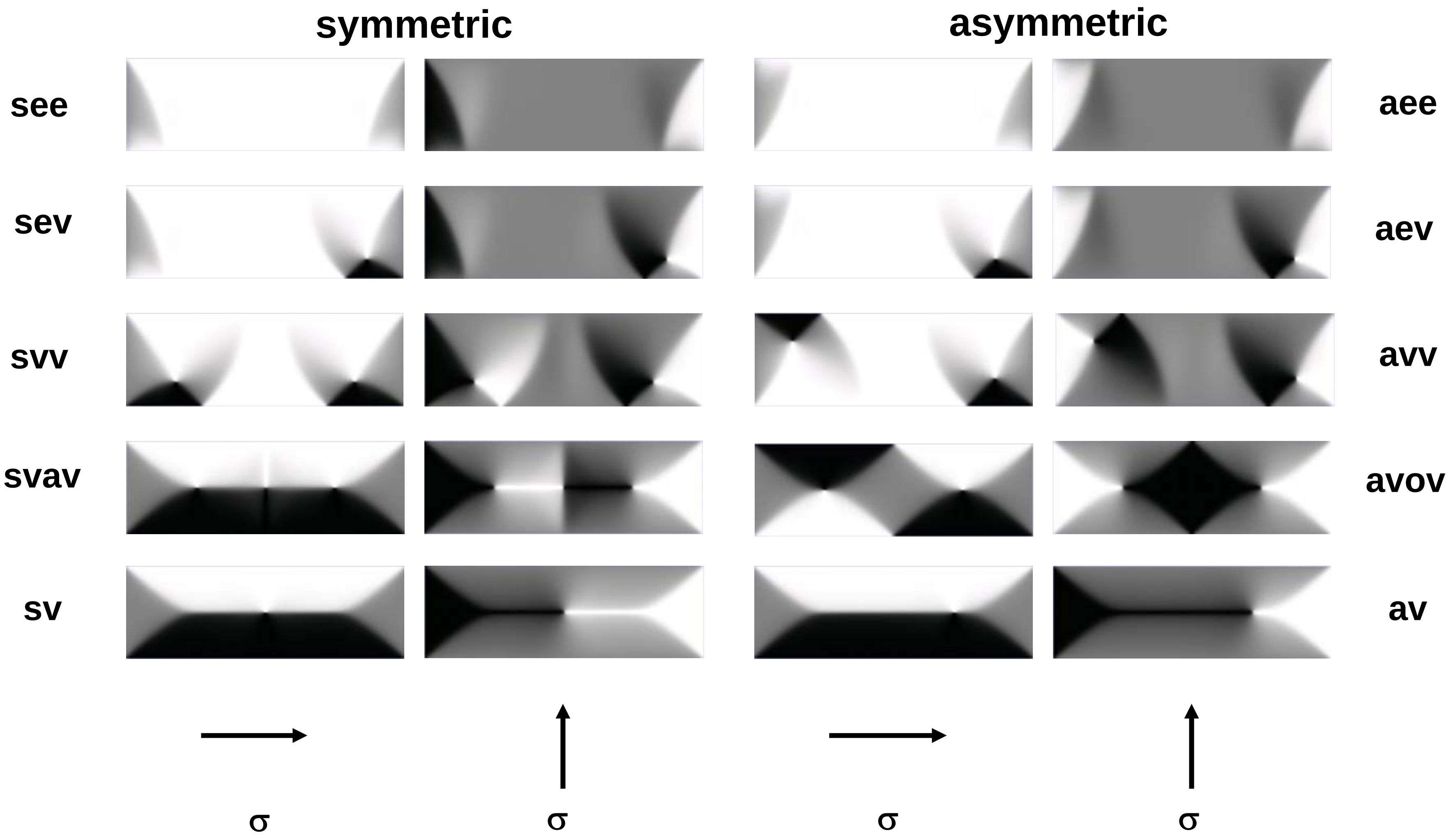

Micromagnetic simulations

R. Hertel, unpublished

1:1

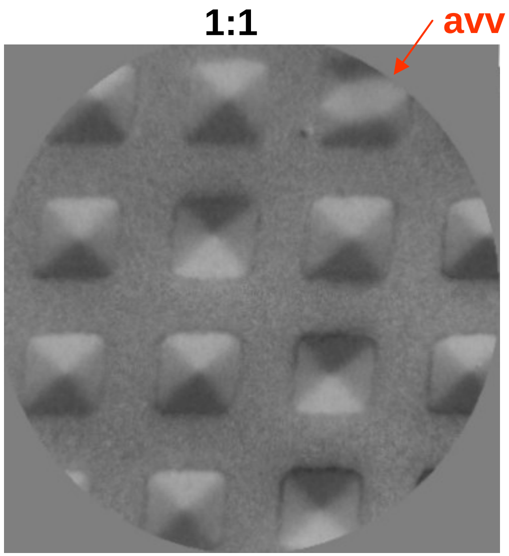

600×600 5 μm

2:1

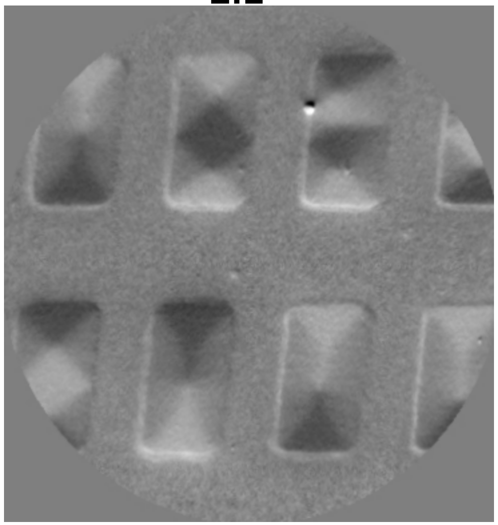

1200×600 5 μm

3:1

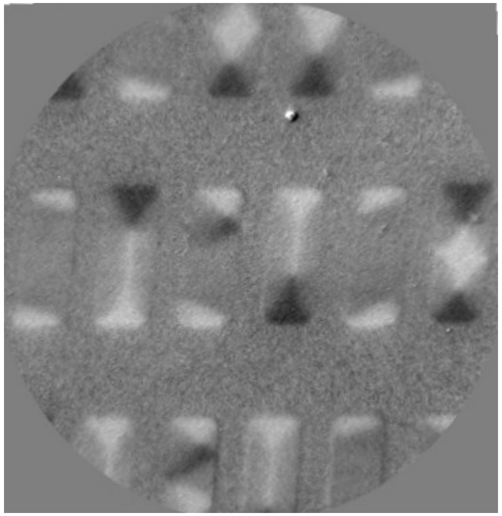

1200×400 5 μm

Energy differences 3:1

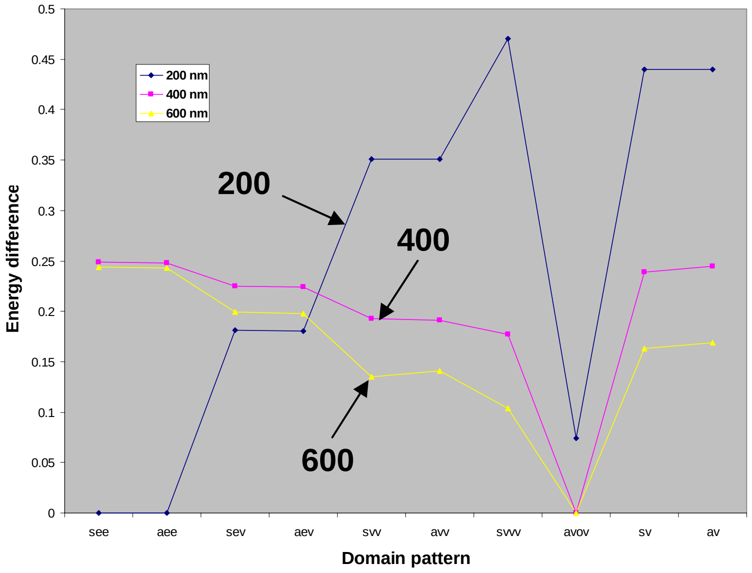

Aspect ratio 3:1

Domain distribution

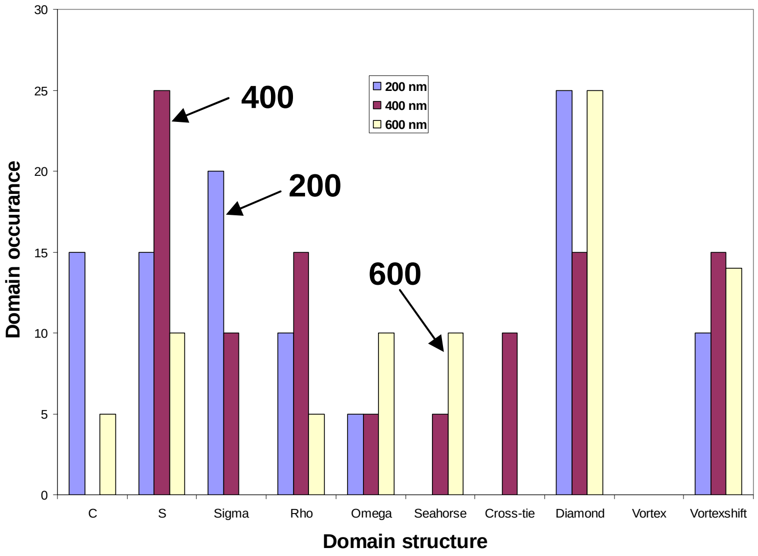

Co 20 nm

Onion States

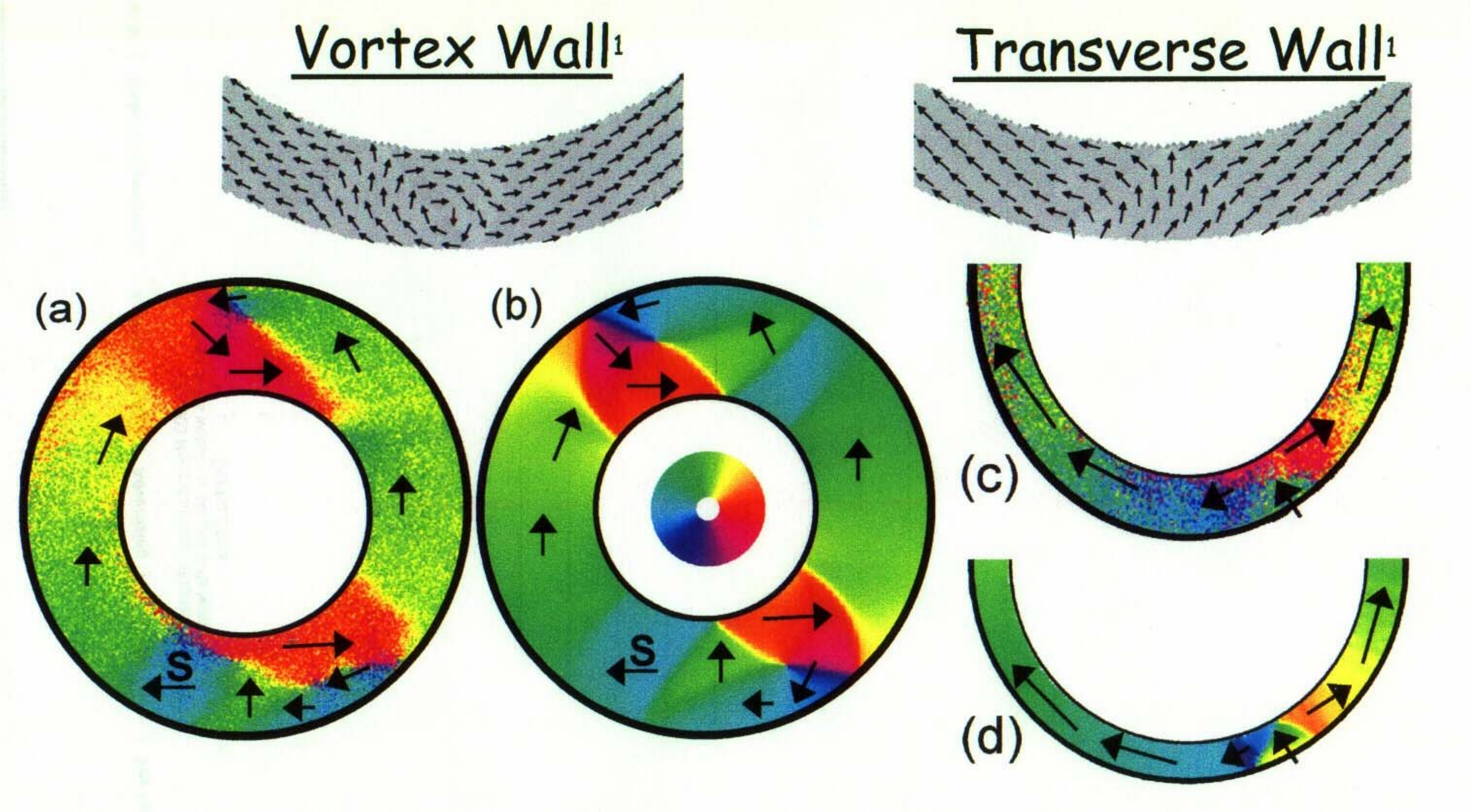

Kläui, priv.commun.

Vortex walls in permalloy rings

1.6 μm O.D.

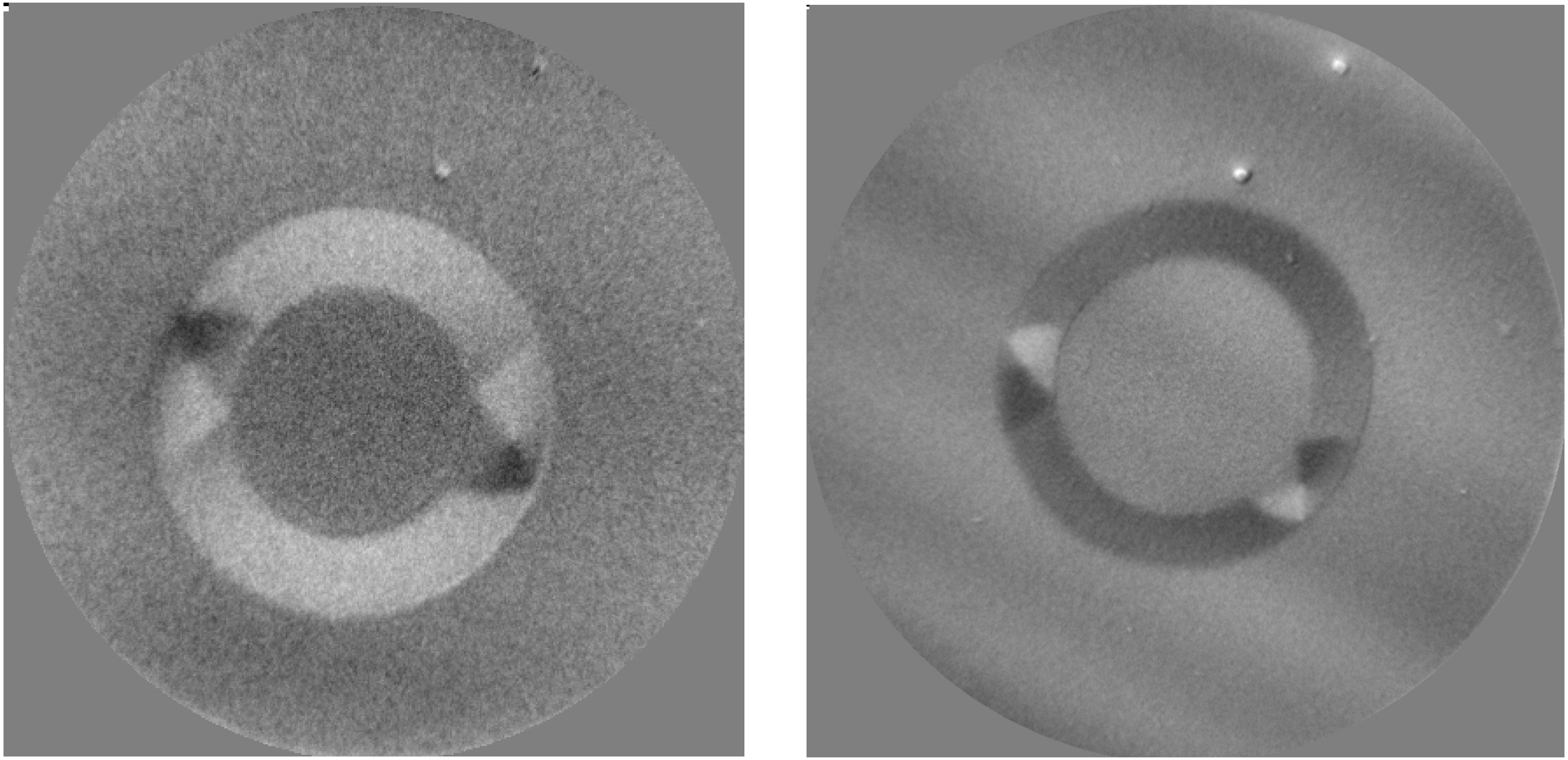

MnAs

Bulk properties

Magnetization

ferromagnetic | paramagnetic

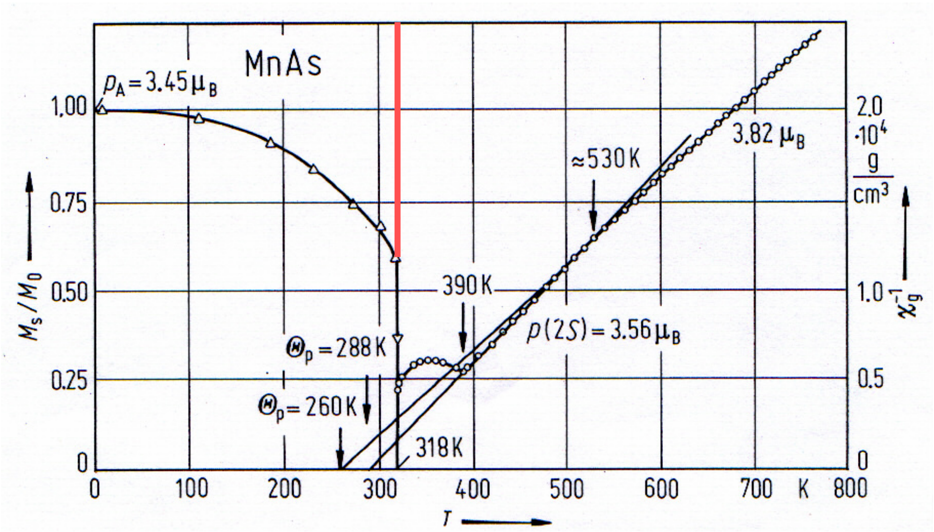

Sudden loss of magnetization
at structural transition

Thermal expansion
a, c, V

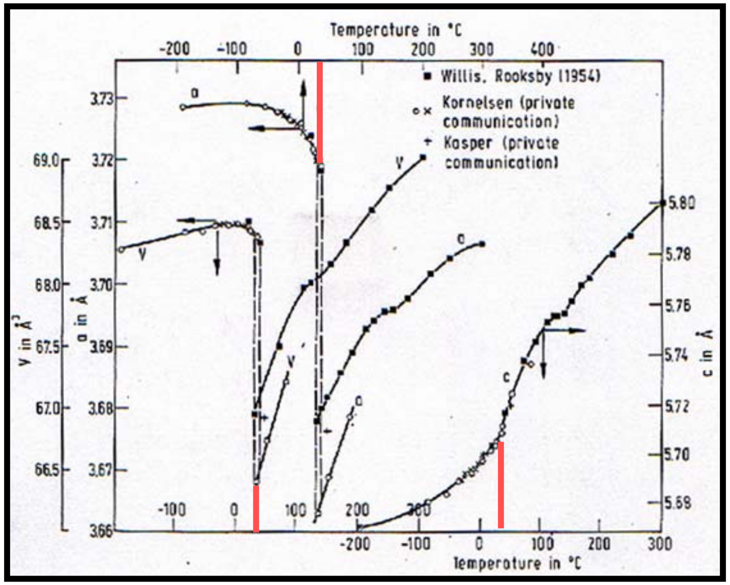

Large a contraction, little c expansion
at phase transition

MnAs

α T< ≈ 40 °C NiAs (hexagonal) ferromagnetic
β MnP (orthorhombic) paramagnetic
γ T > 125 °C NiAs (hexagonal) paramagnetic

MnAs for spin injection into GaAs at room temperature?

Problem: strain-induced phase coexistence between ferromagnetic and paramagnetic phase around room temperature

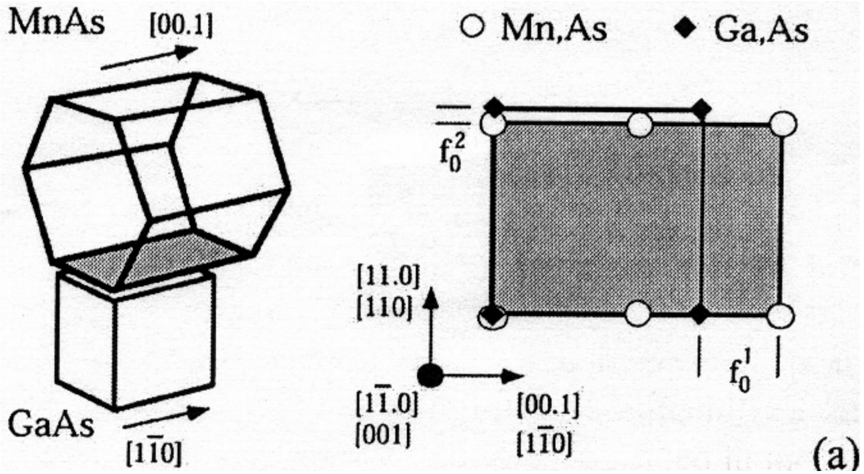

α MnAs / GaAs(100) $f_0^2 = 7.7\%$

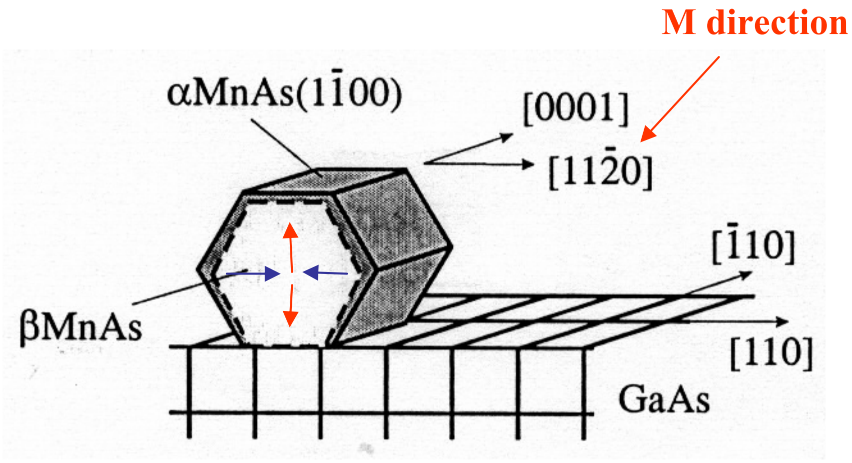

from L. Daeweritz et al ≥ 1999

MnAs on GaAs(100)
Thickness dependence of stripe period
Structural images (LEEM)

Room temperature

Diameter of field of view

10 µm

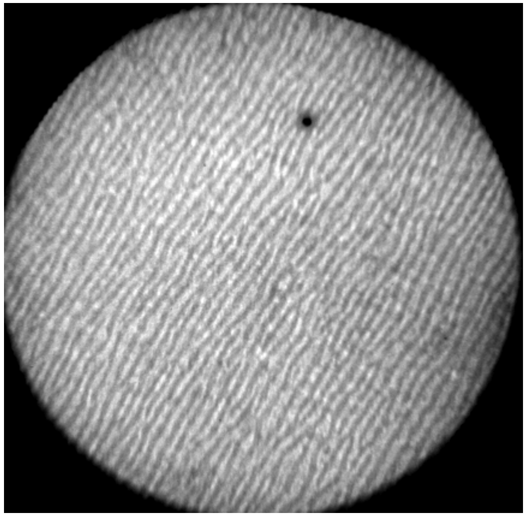

50 nm

10 µm

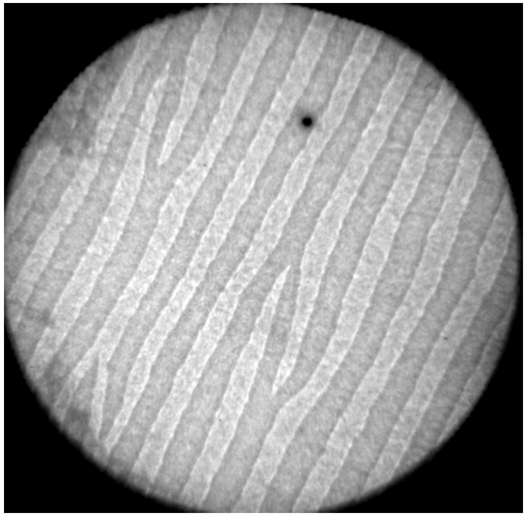

180 nm

5 µm

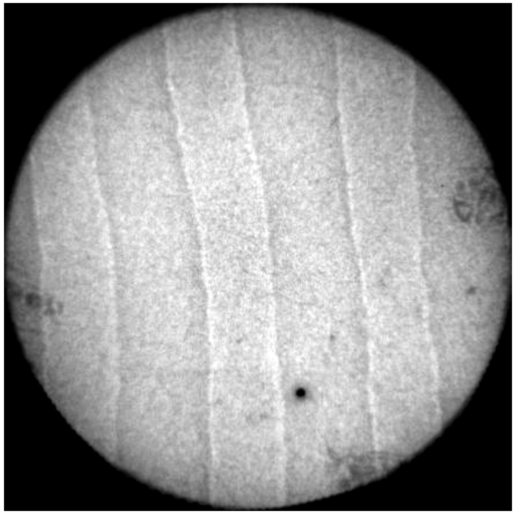

300 nm

MnAs on GaAs(100)

Thickness dependence of magnetic domain structure

Room temperature

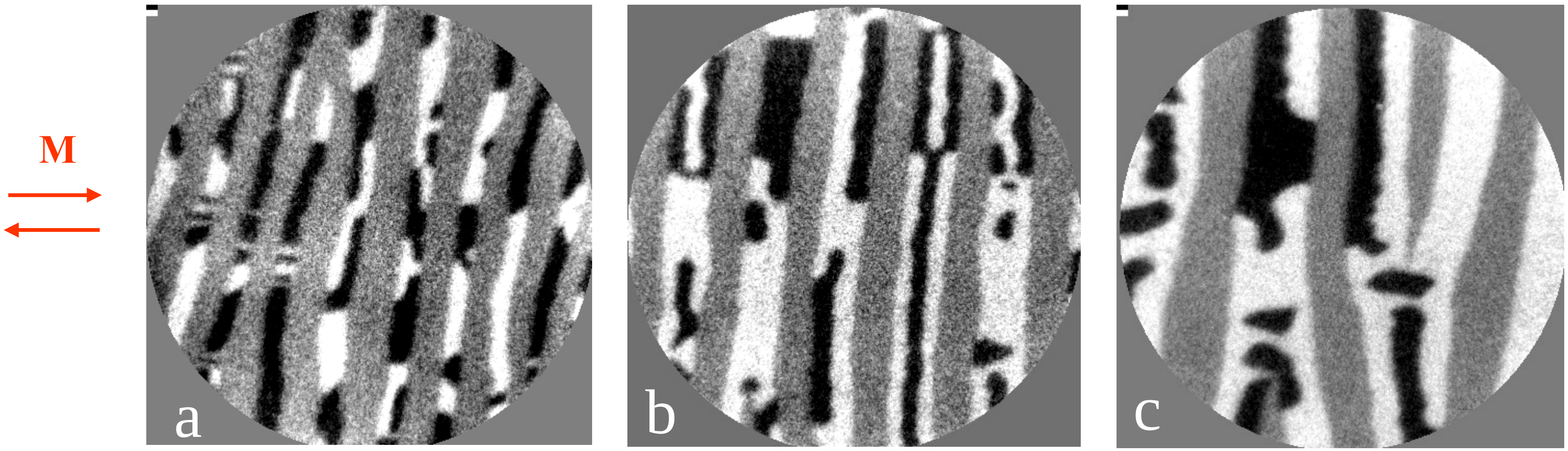

120 nm **180 nm** **300 nm**

Field of view 5 µm diameter

MnAs on GaAs(100)

Phase transition

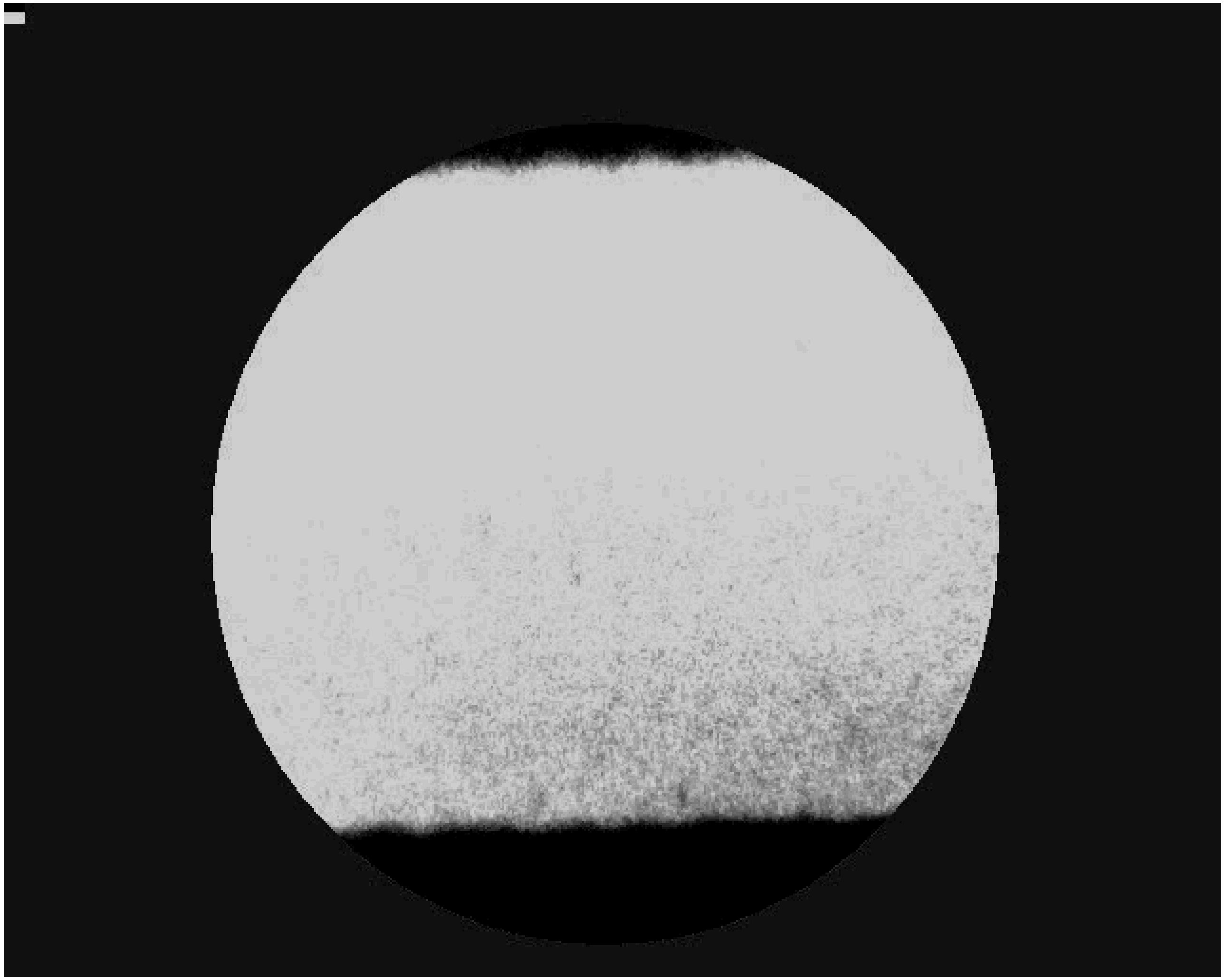

Field of view 5µm diameter

FM (≅ 10°C) → PM (≅ 40°C)

MnAs / GaAs(100) 40 nm

XMCDPEEM Mn $2p_{3/2}$ (639.5 eV)

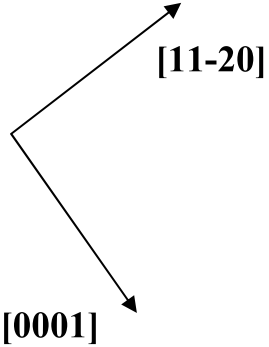

during heating

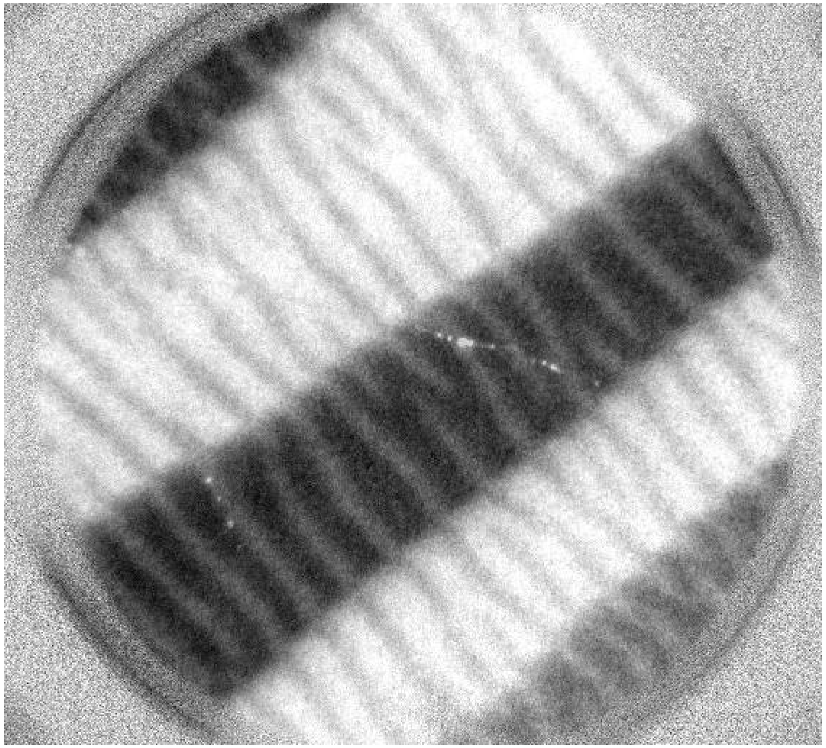

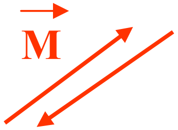

during cooling

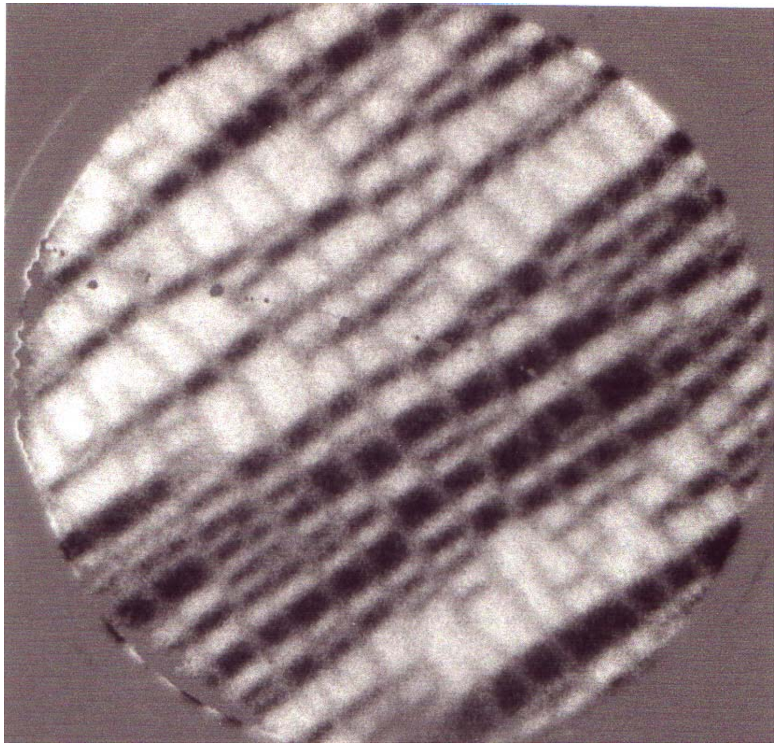

1 µm

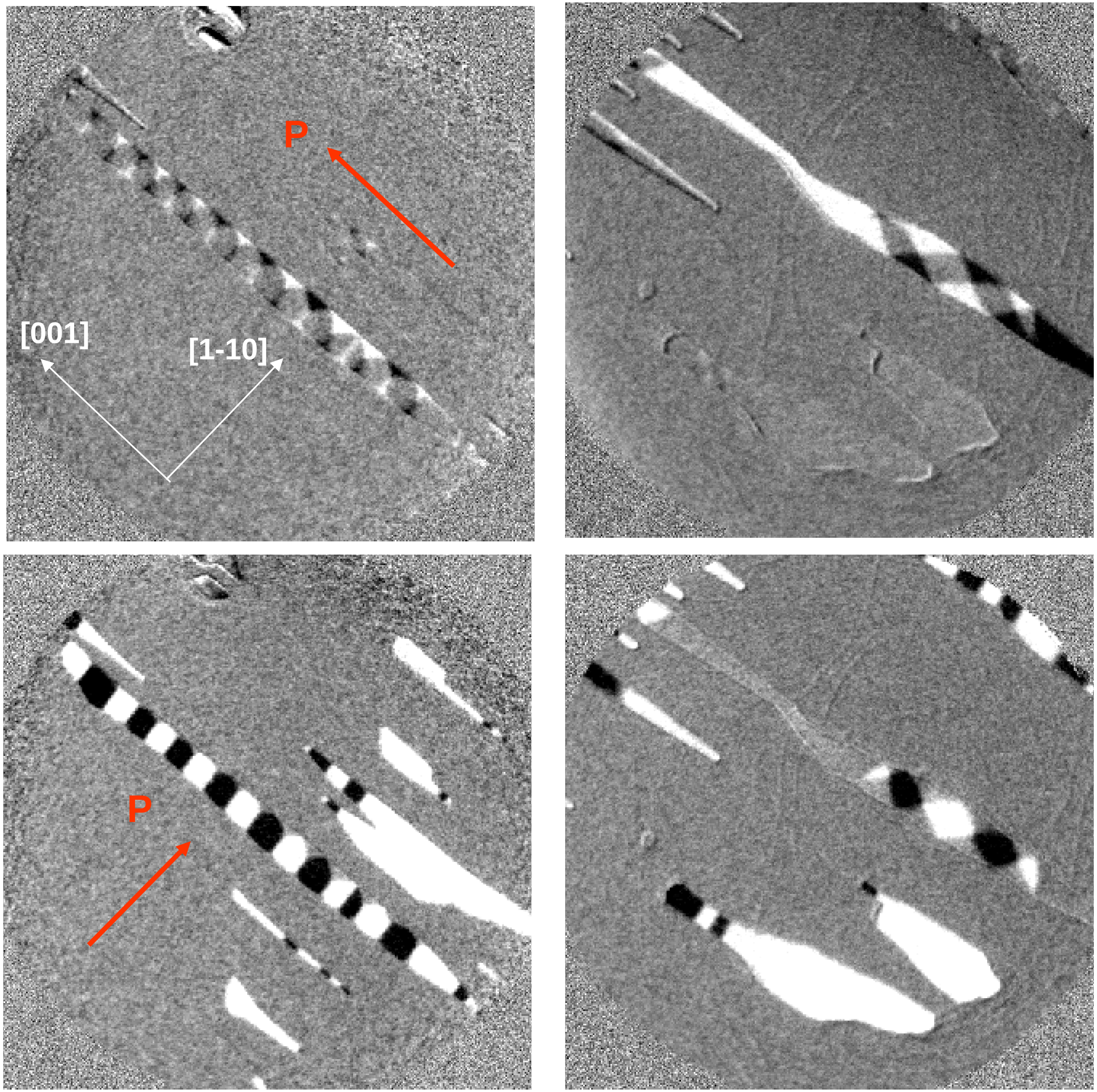

SPLEEM

Domain structure of thin Fe crystals

~5 ML Fe/W(110) deposited at RT and annealed at ~700 K

Field of view:
Left column: 18 μm
Right column: 12 μm.

[001]: hard axis
[1-10]: easy axis

Electron energy:
2.5 eV

R. Zdyb

Spin reorientation transition: $Fe_{0.7}Co_{0.3}$ / Au(111)

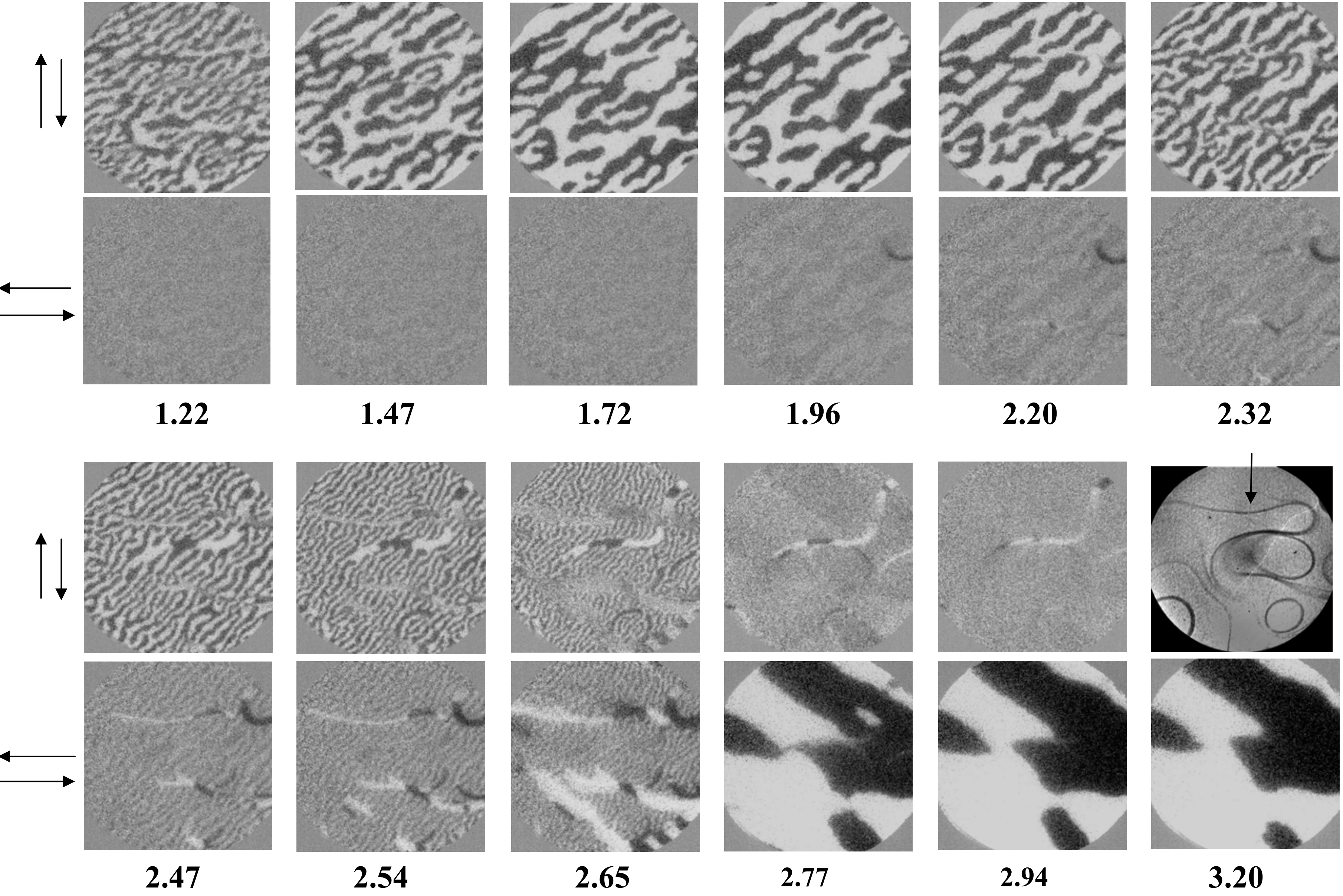

Summary

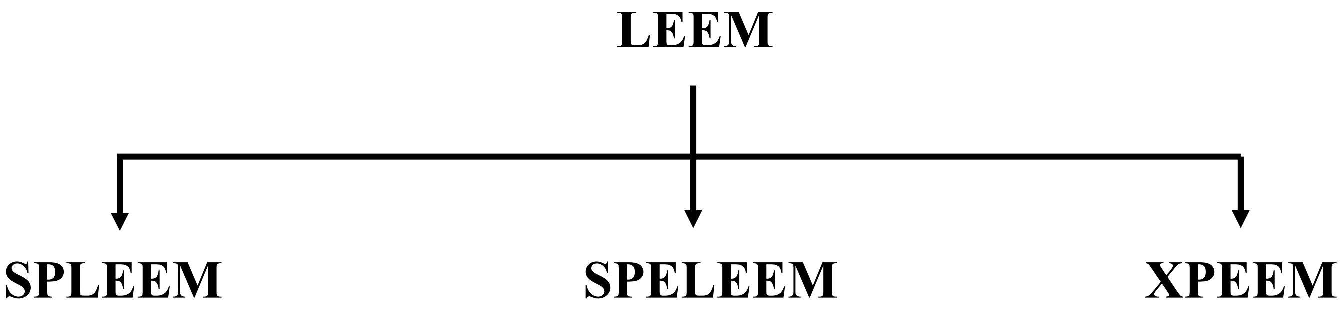

LEEM: 5 nm (FE), 7 nm ($\mathrm{LaB_6}$)
SPLEEM: 20 nm (stability-, noise-limited)
SPELEEM: 10 nm (in LEEM), 25 nm (in SE-XPEEM),
50 nm (in XMCDPEEM, stability-, noise-limited)
XPEEM: 10 nm?

Aberration correction (SMART, PEEM III):
1 nm?